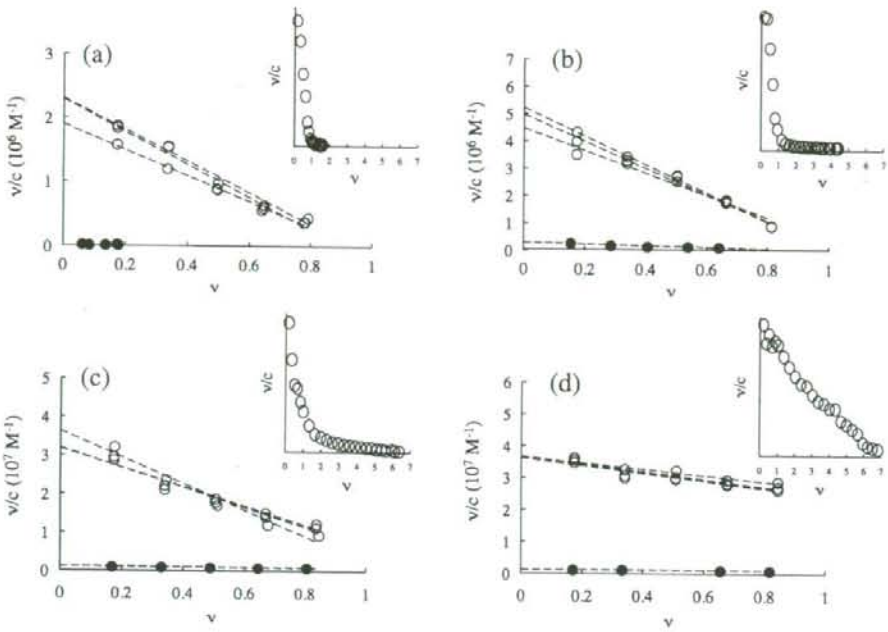

Figure 1. Albumin binding of octanoate (a), decanoate (b), laurate (c) and myristate (d). Main parts show binding to HSA (○) and to the recombinant mutant R410A (●). The symbols represent single determinations. The insets show binding of higher fatty acid concentrations to HSA. These symbols (○) represent average values for five to ten experiments. ν stands for the number of mol of fatty acid bound per mol of protein, whereas c is the concentration of unbound fatty acid anion.

to[24,25], or slightly lower than,[23] those previously published. From the inset to Figure 1(d), it is seen that the binding curve for myristate is very different from those characterizing binding of the other three fatty acids with a shorter chain length. The binding curve for myristate is less steep at low ν-values, and it has also a much less clear tendency to flatten out. In addition, the flattening out takes place at a higher ν-value, namely at $\nu \sim 2$. These findings indicate, as suggested in the literature,[18,21,25] that the first two molecules of myristate bind to HSA with high affinities, but also that binding of the following molecules takes place with only slightly lower affinities.

The above findings indicate significant differences in the modes of interaction between albumin and the four medium-chain fatty acids. As illustrated by the K_1-values, the binding affinities are dependent on the size of the hydrophobic part of these ligands, a finding that attests to the importance of non-polar forces for binding. However, the increase in the K_1-values is not directly related to chain length: K_1 for laurate is 6.7 times that determined for decanoate, whereas the ratios between K_1 for decanoate/octanoate and myristate/laurate are only 2.6 and 1.1, respectively. Principally the same observation was made by Ashbrook *et al.*, and it can probably be explained by varying degrees of configurational adaptability of the albumin binding sites as the fatty acid increases in length.[21] Tanford has estimated the free energy of association between anionic, aliphatic amphiphiles (carboxylates, sulfates and sulfonates) and native bovine serum albumin.[26] He found that the free energy was linearly dependent on hydrocarbon chain length for ligands having up to eight carbon atoms. By contrast, the free energies of binding were less than expected for amphiphiles of a longer chain length. Tanford explained these findings by assuming size limitation of the binding sites. However, the present observations, and those of Ashbrook *et al.*[21] and Tanford,[26] can perhaps also be explained by a third mechanism, i.e. by fatty acid binding to different regions of the albumin molecule. In any case, the observations show that binding of fatty acids to albumin is not a simple function of chain length.

Fatty acid binding sites of HSA

The most detailed description of fatty acid binding to HSA has been obtained by X-ray diffraction studies of recombinant HSA co-crystallized with specific fatty acids.[6–8] Unfortunately, these investigations did not include binding studies with octanoate. Figure 2(a) shows HSA complexed with decanoate as well as the subdivision of the protein into domains (I – III) and subdomains (A and B). By using a large fatty acid to protein molar ratio it was possible to identify ten binding sites for decanoate (number 1–9 plus 6′). Different types of locations were found, namely sites within subdomains (1, 4 and 7), sites involving residues from more than one subdomain (2, 3, 5, 6 and 6′), and sites placed

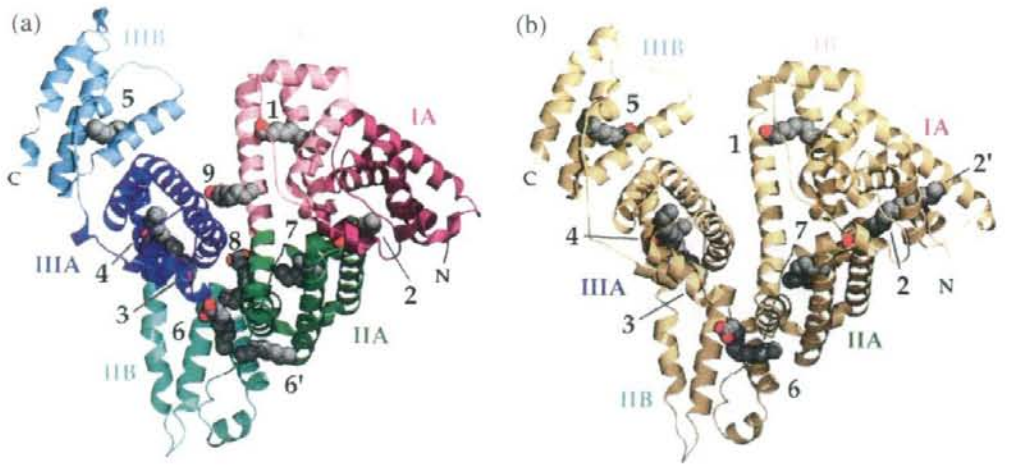

Figure 2. Crystal structure of rHSA complexed with decanoate (a) or laurate (b). The structures reveal ten decanoate binding sites and eight laurate binding sites. The numbering of the sites is taken from Bhattacharya *et al.*[8] The fatty acid anions are depicted in space-filling representation; oxygen atoms and carbon atoms are colored red and grey, respectively. The subdivision of rHSA (and HSA) into domains (I–III) and subdomains (A and B) is indicated. N and C represent the N terminus and C terminus, respectively. The illustrations were made with Molscript on the basis of the atomic coordinates 1e7e (a) and 1e7f (b) available at the RCSB Protein Data Bank.

between subdomains (8 and 9). Of these sites, Sites 6 and 6′are situated on the surface of HSA. Only eight sites were detected for laurate (Figure 2(b)) and myristate (not shown), namely Sites 1–7 with the same locations as found for decanoate and a new site (2′) placed in subdomain IA. In the following, the site numbering of Figure 2 will be used. Although the studies referred to[6–8] are a great step forward in our understanding of fatty acid binding to HSA, they are not able to distinguish high-affinity sites from sites with a lower affinity. However, a hint can be found in the case of myristate binding, because only Sites 1–5 were detected using a lower fatty acid to protein molar ratio.[6]

In vivo, albumin is a complex molecule carrying out its functions in aqueous solutions. Therefore, for getting a more complete understanding of the proteins ability to, for example, interact with aliphatic fatty acids it is necessary to perform supplementary studies with albumin in solution. For that purpose, NMR spectroscopy would be useful, but the high molecular mass and helical content of HSA is still a problem to that kind of investigation. Here, we have attempted to throw light on the fatty acid binding properties of HSA by site-directed mutagenesis. When selecting positions for mutagenesis we used the X-ray structures described by Bhattacharya *et al.* (Figure 2) as a guide.[8] For mutagenesis we chose ten important residues in the fatty acid binding sites 1, 4, 5 and 7, and the mutated residues are shown in greater detail in Figure 3.

Recombinant HSA mutants

The 12 single-residue mutants, the single double-residue mutant and wild-type rHSA were produced using a yeast expression system. Before freeze-drying, all the isolated proteins were treated with charcoal and dialyzed extensively against deionized water for removing any hydrophobic and hydrophilic ligands, respectively. All the albumins were analyzed by far-UV and near-UV CD spectroscopy, and we observed no differences between the spectra for commercial HSA, wild-type rHSA and the mutants. The spectra for most of the proteins have been presented before,[27–29] but the mutants R117A, H146A and Y401A were studied as a part of the present work (not shown). Likewise, the light absorbance spectra (250–350 nm) of all the albumins were comparable (not shown). Thus, the mutations have probably not caused major differences in albumins secondary or tertiary structures.

Fatty acid binding to rHSA mutants

Earlier studies have shown competitive binding of octanoate and diazepam to a common high-affinity site in HSA.[15] Very recently, crystallographic analyses revealed the existence of only one binding site for diazepam, namely a site placed in subdomain IIIA, where the drug interacts with the hydroxyl group of Tyr411 and some hydrophobic residues.[11] Therefore, high-affinity binding of octanoate most probably also takes place in that subdomain, e.g. in Site 3 or 4 reported for binding of fatty acids of a longer chain length (Figure 3(c)). Such an assignment is supported by the observations done in the present study with mutants. Figure 4(a) shows that mutating Arg410 and/or Tyr411 to alanine decreases K_1 to values that are ≤2% of the original value. These findings can be explained by elimination of a salt-bridge between Arg410 and/or a hydrogen bond between Tyr411 and the carboxylate

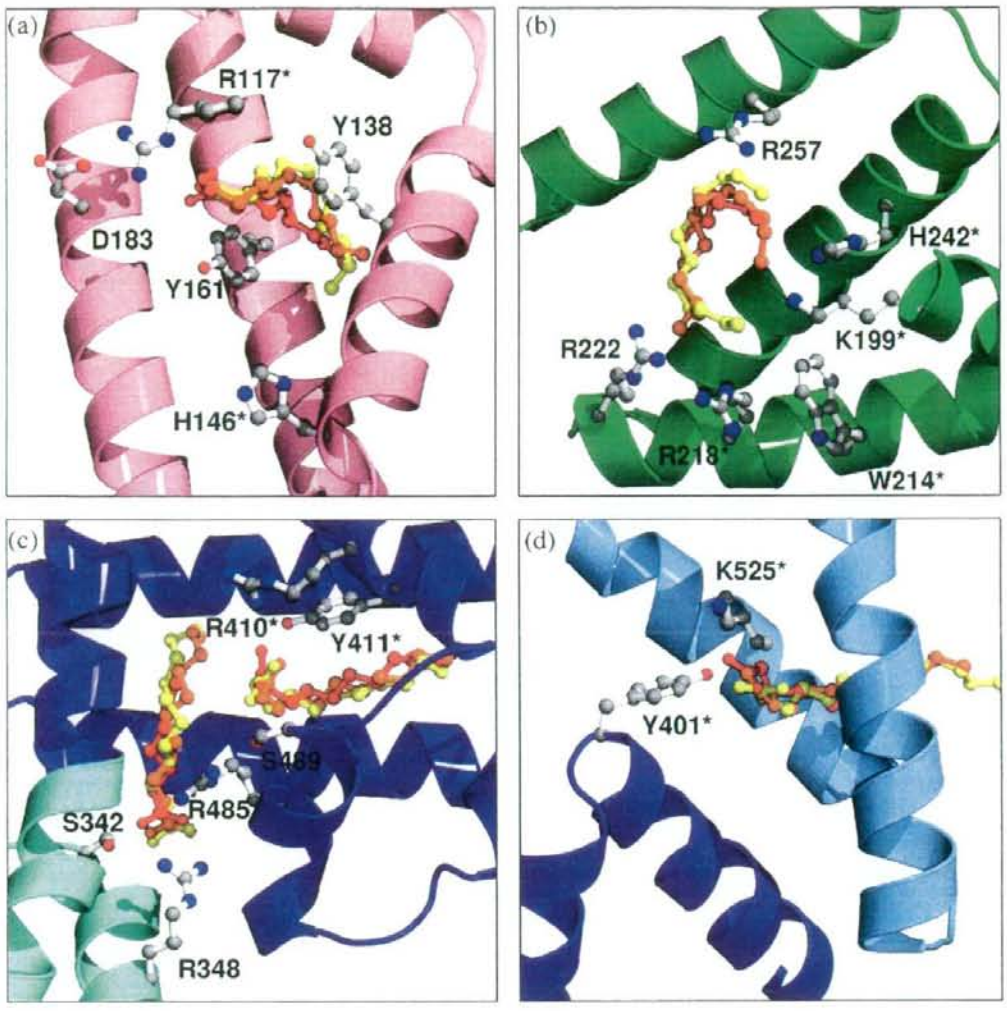

Figure 3. Fatty acid binding to Site 1 in subdomain IB (a), to Site 7 in subdomain IIA (b), to Sites 3 and 4 in subdomains IIB and IIIA (c), and to Site 5 in subdomains IIIA and IIIB (d). The fatty acids are decanoate (red), laurate (orange), and myristate (yellow). The color code for domains and subdomains is the same as that used in Figure 2(a). The residues mutated in this work are marked with an asterix. The illustrations were made with Molscript on the basis of the atomic coordinates 1e7e (decanoate), 1e7f (laurate), and 1e7g (myristate) available at the RCSB Protein Data Bank.

group of the fatty acid,[8] suggesting binding of octanoate to Site 4 (Figure 3(c)). It is widely accepted that the site is adaptable and can undergo ligand-induced alterations. However, substituting Tyr411 with its OH-group to which octanoate can establish a hydrogen bond with serine, which also possesses an OH-group, greatly diminishes binding affinity (Figure 4(a)). Finally, mutating Tyr411 to the hydrophobic phenylalanine has a less dramatic effect on binding.

Surprisingly, mutations in other subdomains of rHSA also decrease K_1 for octanoate binding. Figure 4(a) shows that mutations in fatty acid Site 1 (R117A, H146A), Site 7 (K199A, W214A, R218H, H242Q) and Site 5 (Y401A, K525A) also diminish primary octanoate binding. However, taken as small groups of mutations, as indicated in Figure 4, octanoate binding is mostly affected by the mutations in Site 4. The effects of mutating residues in Sites 1, 5 and 7 are probably not due to abolished octanoate binding to a secondary site(s), because secondary binding only contributes very little to octanoate binding (cf. Figure 1(a), inset). Rather, they are caused by minor, but apparently widespread, conformational changes in the albumin structure. These conformational changes could not be detected by using CD or light absorbance spectroscopy. However, albumin in solution is not a static structure but a molecule changing between different conformational states. The conformational changes involve both small-amplitude fluctuations and large-amplitude fluctuations ("breathing"), and the latter type of changes

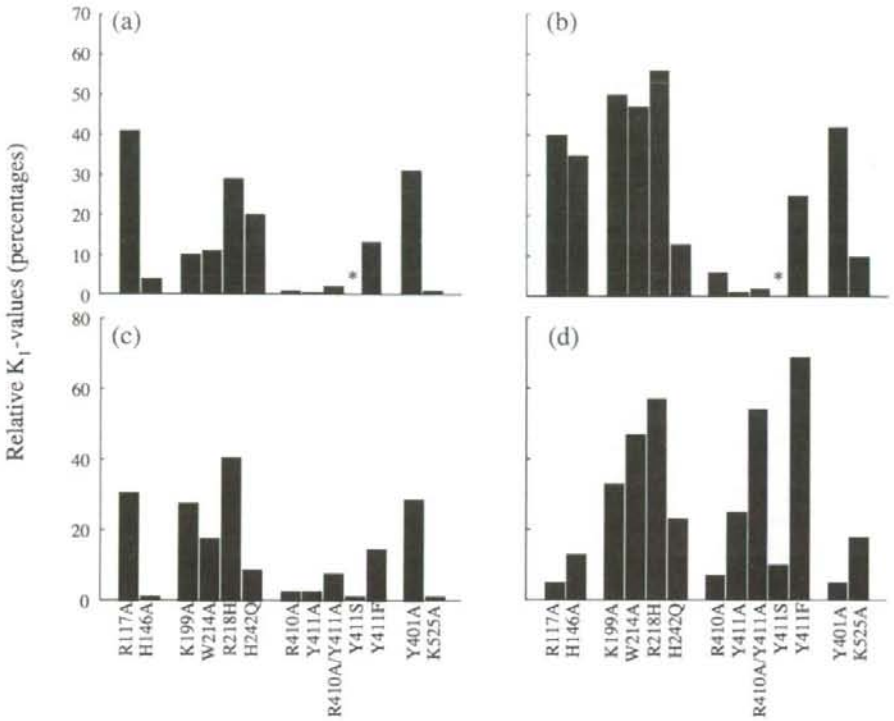

Figure 4. Primary binding of octanoate (a), decanoate (b), laurate (c) and myristate (d) to rHSA mutants. The results are given as K_1-values for the mutants relative to the K_1-values determined for normal albumin. * The relative K_1-value is less than 0.5%. The K_1-values were determined as illustrated in Figure 1, which shows the results for R410A. The Scatchard plots of the binding of each fatty acid to wild-type rHSA and to the remaining mutants are given in Supplementary Data. From Supplementary Data it can be seen that fatty acid binding to wild-type rHSA and HSA are comparable.

can involve relatively large parts of the protein (reviewed by Kragh-Hansen[12]). Thus, even though the two spectroscopic methods could not register any mutation-induced conformational changes, they could still be the explanation for the observed cases of diminished high-affinity binding of octanoate. To our knowledge, these results are the first reported examples of mutation-induced conformational changes affecting ligand binding to other subdomains than the one housing the mutation. However, such effects have previously been observed in the case of ligand-induced conformational changes.[12,30] A recent example is that ligand binding to a sub-site of Site I in subdomain IIA mutually affects binding of diazepam and ibuprofen in subdomain IIIA.[31]

The effects of the mutations on primary decanoate binding were principally the same as those observed for octanoate binding (Figure 4(b)), showing why also decanoate most probably binds with high affinity to Site 4 (Figure 3(c)). Thus, the amino acid substitutions R410A, Y411A, Y411S and the double mutant R410A/Y411A all decreased K_1 to less than 6% of the value determined for normal albumin. In this case as well, mutating Tyr411 to a phenylalanine resulted in a less pronounced decrease of K_1. The other mutations also diminished decanoate binding, although generally to a less pronounced extent than when mutating Arg410 and/or Tyr411. Usually, the diminishing effects on decanoate binding were smaller than those observed for octanoate binding. Because hydrophobic interactions are more important for decanoate binding than for octanoate binding, this finding indicates that formation of hydrophobic interactions are less dependent of the detailed protein structure than, e.g., establishing salt-bridges and hydrogen bonds.

Bhattacharya *et al.*[8] have proposed that Site 7 in subdomain IIA (Figure 3(b)) may be a primary site for shorter-chain fatty acids such as octanoate and decanoate. However, such a proposal is not supported by competition experiments[15] or by the present experimental findings (Figure 4(a) and (b)) which, as argued above, point to Site 4 as the high-affinity site for these fatty acid anions.

Taken as groups of mutations, the mutations in position 410 and 411 have the greatest impact on laurate binding (Figure 4(c)) proposing that also this fatty acid binds with a high affinity to Site 4 (Figure 3(c)). Even though hydrophobic interactions between laurate and HSA must be stronger than those between decanoate and HSA, the effects of the

remaining mutations on laurate binding are more pronounced than the corresponding effects on decanoate binding. This difference is most likely due to the existence of two and not just one high-affinity binding site for laurate. As can be seen from Figure 2, the different effect of the mutations is not caused by an increase in the total number of binding sites for laurate.

Different types of studies with intact albumin and with fragments thereof have proposed the existence of two high-affinity binding sites for long-chain fatty acids such as palmitate and oleate.[7] These sites are probably identical to Sites 1 and 5,[7] with Site 5 having the highest affinity.[7,32] Therefore, even though the two mutations in the two sites have very similar effects on laurate binding (Figure 4(c)), it is tempting to suggest that Site 5 is the additional high-affinity binding site for laurate.

The impacts of the five mutations in position 410 and 411 on myristate binding are principally the same as those observed for the three fatty acid anions of a shorter chain length (Figure 4(d)). However, in the case of myristate the effects are much less pronounced; this is observed especially for Y411F and the double-residue mutant. In addition, the mutations in Site I (K199A, W214A, R218H and H242Q) have only moderate effects on binding. In contrast, all the rHSAs with amino acid substitutions in Site 1 or Site 5 have a greatly diminished affinity for myristate, indicating that the two high-affinity sites for myristate are placed in these sites. Again, Site 5 could represent the highest-affinity binding site. This proposal implies that Site 4 has been "degraded" to a secondary site. As apparent from the following discussion, binding of long-chain fatty acids (e.g. palmitate and oleate) seems to take place according to a similar binding scheme. Thus, high-affinity binding of myristate takes place like fatty acids of a longer chain length and not like laurate and other fatty acids of a shorter chain length.

Kragh-Hansen[12] has proposed, on the basis of ligand competition experiments, an albumin binding model in which the two high-affinity sites for long-chain fatty acids are placed in other regions of the protein than the one binding, e.g., octanoate with high affinity. Using CD spectroscopy, Sjödin registered only a small displacing effect of oleate on HSA-bound diazepam and proposed that the displacement occurred primarily through an allosteric mechanism rather than through direct competition between the two ligands.[33] Cunningham *et al.*[34] found by using an ultrafiltration technique that L-tryptophan binding, taking place to the same site as diazepam,[15] was more decreased by the presence of low concentrations of laurate than by equimolar amounts of palmitate or oleate, even though the latter are bound with much higher affinities. Actually, a marked inhibition of L-tryptophan binding by palmitate and oleate only occurred when their molar ratios to albumin were increased to 2 or above. The binding model is also supported by other types of studies. For example, Koh and Means[35] observed that the esterase-like activity of HSA, which is due to Arg410 and Tyr411,[27] is effectively inhibited by medium-chain fatty acids up to decanoate but not by longer-chain fatty acids.

Very recently, Simard *et al.*[32] investigated the binding of ^{13}C-labeled palmitate and oleate to rHSA and to two mutants thereof by X-ray crystallography and ^{13}C NMR spectroscopy and proposed fatty acid binding to three sites of a high affinity. At a 1:1 molar ratio of fatty acid to albumin two NMR peaks (181.5 and 181.8 ppm) were observed, and a third peak (182.2 ppm) appeared at a 2:1 molar ratio. At higher ratios more peaks appeared. When mutating Lys525 to alanine, one of the first two peaks, the most intense one (181.8 ppm), disappeared or diminished very much, proposing that Site 5 is a high-affinity binding site. The authors also produced a recombinant domain III fragment (residues 382–585), and fatty acid binding to that peptide produced two of the three peaks (181.8 and 182.2 ppm) but not the initial one at 181.5 ppm, suggesting that a high-affinity site is placed N-terminally to domain III. Finally, when mutating both Arg410 and Tyr411 in the intact protein to alanine, the third peak (182.2 ppm), only observed at a molar ratio of 2:1 or higher, disappeared. These results are in full accordance with a binding model proposing Sites 1 and 5 as high-affinity sites and Site 4 as a secondary one, i.e. a binding model similar to that proposed for myristate binding. Simard *et al.*[36] have just expanded their studies on palmitate binding to include drug-competition analyses. The results of these extensive investigations support the binding model except for the assignment of a high-affinity binding site to Site 1 (represented by the peak at 181.5 ppm). From experiments with the R117A mutant and displacement studies with hemin and phenylbutazone the authors suggested that Site 2 and not Site 1 is a high-affinity site. From the present work we cannot exclude that also one of the two high-affinity sites for myristate binding is placed in Site 2 instead of in Site 1, because we have not yet produced mutants in Site 2.

Under normal physiological conditions, albumin carries 0.3–1 mol of fatty acids per mol of protein.[5] At such molar ratios, the fatty acids mainly bind to their respective high-affinity sites. Therefore, it is of physiological, pharmaceutical and pharmacological importance to have some knowledge about the location of these sites, because such knowledge can be useful when predicting potential ligand interactions. For example, our results showed that high-affinity binding of long-chain fatty acids, but not high-affinity binding of octanoate and decanoate, could take place in Site 1 to which also heme binds with a high affinity.[30] Furthermore, in contrast to high-affinity binding of long-chain fatty acids high-affinity binding of octanoate and decanoate takes place to Site 4 and thereby will compete with high-affinity binding of drugs like

diazepam, ibuprofen, diflunisal, halothane and propofol.[11]

Crystallographic analyses of fatty acid–albumin complexes were not able to determine the locations of the carboxylate head-groups and the methyl ends of fatty acids bound in Site 7, while their orientation in that site still is unknown (Figure 3(b)).[8] Unfortunately, the present work with recombinant mutants is not able to solve that problem, because binding to Site 7 is low-affinity binding, which does not contribute much to total binding at the molar ratios used here.

Fatty acid binding to natural mutants of HSA

We were surprised to see, that all the recombinant mutations decreased primary fatty acid binding (Figure 4); no example of unmodified or increased binding was found. Does this mean that fatty acid binding to albumin is so sensitive that all mutations will affect binding? In an attempt to throw some light on that question we have collected qualitative information for laurate binding, as an example, to genetic variants of HSA. As seen from Figure 5, 11 of 13 single-residue mutations had no or only a very small effect on binding, whereas one increased binding and one decreased binding. Thus, it is not obligatory that albumin mutations affect fatty acid binding.

Genetic variants of HSA (alloalbumins) are usually found by electrophoresis under non-denaturing conditions. This implies that the substitutions are located on the surface of the protein molecule and are exposed to the solvent. Therefore, the importance of mutations for fatty acid binding could be so that most of the mutations at albumins surface do not effect binding (Figure 5), whereas mutations in the inner parts of the protein, e.g. in binding sites, usually affect binding (Figure 4).

Concluding remarks

The K_1-value for binding of octanoate, decanoate, laurate and myristate increases with the chain length of the fatty acid, reflecting the importance of hydrophobic effects for binding. Furthermore, the number of high-affinity binding sites and their location in the albumin molecule most probably also depend on the chain length. Thus, octanoate and decanoate bind to Site 4. By contrast, both laurate and myristate seem to bind to two high-affinity sites, namely Sites 4 and 5 and Sites 1 and 5, respectively (Figures 2 and 3). The results obtained with the recombinant mutants and with genetic variants show that fatty acid binding is influenced by amino acid substitutions in the interior of the protein but much less so by mutations of superficially placed amino acid residues.

Binding of fatty acid anions to different high-affinity sites, and the sensitivity of the sites to amino acid substitutions elsewhere in the protein (and perhaps also to other types of modifications) are important factors in cases of simultaneous binding of other ligands. These circumstances have to be taken into account, e.g., when patients are treated with albumin-binding drugs.

In the present work, most of the focus has been on K_1-values. This was done for making interpretations somewhat less complicated. Furthermore, under physiological conditions HSA only carries one mol, or less, of fatty acid anion per mol of protein.

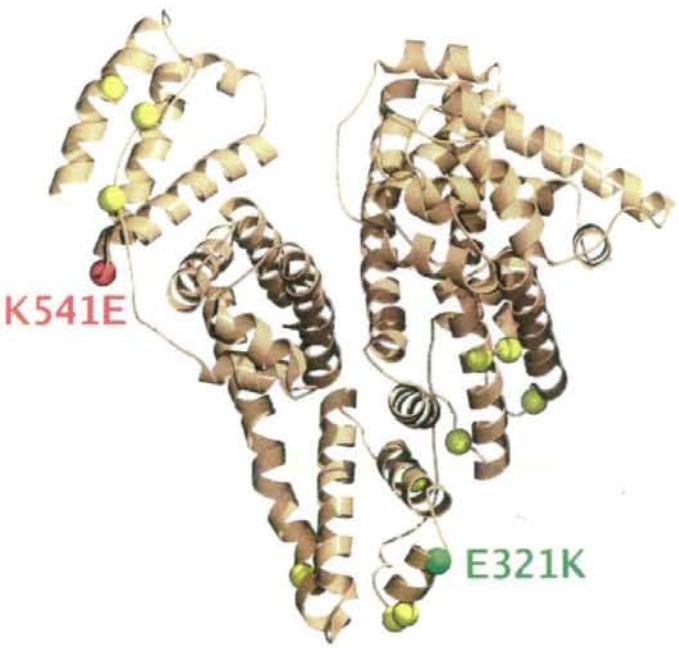

Figure 5. Laurate binding to natural mutants of HSA. Mutation of the residue in green (E321K) and of the one in red (K541E) results in increased and decreased fatty acid binding, respectively. Residues in yellow indicate that substitution of these amino acids does not affect binding much or not at all; the mutations are K225N, K240E, D269G, K276N, K313N, D314V, E333K, K372E, E501K, E505K and K573E. The information is from published[37,38] and unpublished (D314V) observations. The illustration was made with Molscript on the basis of the atomic coordinates 1ao6 available at the RCSB Protein Data Bank.

Materials and Methods

Materials

HSA (A-1887, >96% pure and essentially fatty acid free (less than 0.01 mol/mol albumin, according to the manufacturer)) was obtained from Sigma Chemical Co. (St. Louis, MO, USA). The DNA techniques for producing wild-type rHSA and mutants thereof, using the yeast species *P. pastoris* (strain GS115) as an expression system, have been published.[27,28] The mutagenic primers used for the mutants R410A, Y411A, Y411S, Y411F and for the double-residue mutant R410A/Y411A have been presented,[27] and those used for the single-residue mutants K199A, W214A, R218H and H242Q have been published.[28] Additional mutagenic primers used (underlined letters indicate mismatches) were 5′-CCCCCGATTGGTGGCACCAGAGGTTGATG-3′ for R117A, 5′-GCCAGAAGAGCTCCTTACTTTTATGCCC-3′ for H146A, 5′-GCTTGGAGAGGCCAAATTCCAGAATGCGC-3′ for Y401A and 5′-GACAAATCAAGGCACAAACTGCAC-3′ for K525A. In all cases, the DNA sequence of the entire albumin coding region was verified as described.[27,28] Secreted albumin was isolated from the growth medium and purified as usually done.[27,28] For removing any hydrophobic ligands, the albumins were treated with charcoal at pH 3 as described by Chen,[39] deionized, freeze-dried and then stored at −20 °C until use. The recombinant albumins (treated with dithiothreitol) exhibited a single band on SDS/PAGE, and they all migrated to the same position as HSA. Density analysis of protein bands stained with Coomassie Brilliant Blue showed that the purity of the recombinant albumins was better than 97%. The molecular masses of all the albumins were taken to be 67 kDa.

Octanoic acid (sodium salt) was from Merck (Hohenbrunn, Germany), *n*-decanoic acid was from Sigma, whereas lauric acid and myristic acid were from Fluka Chemika (Buchs, Switzerland). [1-^{14}C]Octanoic acid (53 Ci/mol) and [1-^{14}C]decanoic acid (55 Ci/mol) were from American Radiolabeled Chemicals Inc. (St. Louis, MO, USA), whereas [1-^{14}C]lauric acid (57 Ci/mol) and [9,10(*n*)-^{3}H]myristic acid (54 Ci/mmol) were from Amersham Life Science (Little Chalfont, Buckinghamshire, UK). Other chemicals were also of the best grades commercially available, and all solutions were prepared in doubly deionised water.

Intrinsic CD spectra

Far-UV intrinsic spectra were recorded from 200 to 250 nm using a protein concentration of 1.5 μM in 66 mM sodium phosphate buffer (pH 7.4, 25 °C). Near-UV spectra were obtained from 250 to 350 nm at a protein concentration of 15 μM in the same buffer. All measurements were made with a Jasco J-720 type spectropolarimeter (Tokyo, Japan).

Spectrophotometry

The light absorbance spectra of HSA, rHSA and the mutants (20 μM) dissolved in 66 mM sodium phosphate buffer (pH 7.4) at room temperature were recorded from 250 nm to 350 nm using 1 cm quartz cuvettes and a Shimadzu UV-160A Spectrophotometer (Kyoto, Japan).

Fatty acid binding

Buffered solutions of the fatty acid anions, with or without a small fraction radiolabeled, were prepared; some of the solutions were with albumin. The medium was in all cases 66 mM sodium phosphate (pH 7.4) with 10 mg gentamicin sulfate added per liter at 25 °C. Control experiments revealed that the antibiotic did not interfere with binding. The albumin concentration (30 μM) was determined by dissolving a weighted amount of the protein in the desired volume of buffer and checking spectrophotometrically at 279 nm using the absorbance at 1 mg/ml of 0.531.[1] When studying ligand binding to HSA, the total fatty acid concentrations varied from 5 μM to 210 μM. The binding experiments including the recombinant proteins were carried out with lower total ligand concentrations, namely 5–25 μM.

Binding was quantified by the kinetic dialysis technique described.[13] In short, two types of experiments were performed. For the first type, buffered solutions of 25 μM fatty acid anion, with or without radiolabeled traces, were made. At time zero, 1.0 ml samples of the former and latter type of solutions were pipetted into left and right compartments, respectively, of 2.4 ml Plexiglas cells. Each cell was divided into two equal compartments by a cellulose membrane cut from dialysis tubing (Union Carbide Corp., Chicago, IL, USA). After closure, the filled cells were rotated in a cabinet having a constant temperature of 25 °C. After 5, 10, 15, 20, 25 or 30 min the half-cells were emptied, and 750 μl portions from the left and right compartments were used for liquid-scintillation counting in a Packard Tri-Carb spectrometer.

In the second type of experiments, solutions of different concentrations of fatty acid were prepared with or without radiolabeled fatty acid included. However, these solutions also contained a constant quantity of albumin. At time zero, 1.0 ml samples of the former and latter type of solutions were pipetted into the left and right compartments, respectively, of the dialysis cells. These cells were allowed to rotate in the cabinet for a known time of approximately 3 h (octanoate and decanoate) or 19 h (laurate and myristate). After the half-cells had been emptied, aliquots of 750 μl were taken for liquid-scintillation counting. Because the stock solutions of decanoate, laurate and myristate for both types of experiments were prepared in 4 mM NaOH, the pH of the final solutions was checked at room temperature.

Calculations

In both types of experiments, the time of dialysis was insufficient to establish equilibrium with respect to the radioactive label. Therefore, it is possible to calculate, from the experiments performed without protein, a rate constant, k, for net transfer of unbound fatty acid anion through the dialysis membrane from the following relationship:[13]

$$\ln\left[\frac{Q_l - Q_r}{Q_l + Q_r}\right] = -k \times t \qquad (1)$$

The terms Q_l and Q_r stand for radioactivity in the samples taken from the left and right compartments, respectively, after dialysis for t min. Now, knowing k for unbound ligand, it is possible to determine the concentration of

unbound fatty acid anion, c, in the albumin-containing solutions:[13]

$$\ln\left[\frac{Q_i - Q_r}{Q_i + Q_r}\right] = -k \times t \times \frac{c}{C} \quad (2)$$

In equation (2), C denotes the known concentration of total ligand. Performing experiments with different concentrations of total ligand gives connected values of c and v; the latter parameter is the number of mol of fatty acid anion bound per mol of protein.

Applying the following equation to the different sets of binding data, v and c, allows a calculation of stoichiometric association constants, i.e. K_1, K_2,..., K_N:

$$v = \frac{K_1c + 2K_1K_2c^2 + \ldots + NK_1K_2\cdots K_Nc^N}{1 + K_1c + K_1K_2c^2 + \ldots + K_1K_2\cdots K_Nc^N} \quad (3)$$

The term N represents the maximum number of ligand molecules that can be bound per albumin molecule.

An estimate of the first stoichiometric constant, K_1, can be obtained by a simple graphical approach. Dividing equation (3) by c leads to:

$$\frac{v}{c} = \frac{K_1 + 2K_1K_2c + \ldots + NK_1K_2\cdots K_Nc^{N-1}}{1 + K_1c + K_1K_2c^2 + \ldots + K_1K_2\cdots K_Nc^N} \quad (4)$$

From equation (4) it is seen, that if $c \rightarrow 0$ (or $v \rightarrow 0$) then $v/c \rightarrow K_1$. In practice, the experimental data are plotted as a Scatchard plot, v/c *versus* v, and K_1 is obtained by extrapolation of v to 0.[13]

Calculations of rate constants, k, and binding constants, K_1, were performed by an iterative procedure with the Sigma Plot software from Jandel Scientific, which enables linear regression with confidence intervals.

Acknowledgements

We thank Dr Anders O. Pedersen for help with the experimental work and Dr Morten Kjeldgaard for help in making the molecular illustrations. This work was supported, in part, by Fonden af 1870 and by Grants-in-Aid for Scientific Research from the Ministry of Education, Science, Sports and Culture of Japan (14370759).

Supplementary Data

Supplementary data associated with this article can be found, in the online version, at doi:10.1016/j.jmb.2006.08.056

References

1. Peters, T., Jr (1996). All About Albumin: Biochemistry, Genetics, and Medical Applications. Academic Press, San Diego.
2. He, X. M. & Carter, D. C. (1992). Atomic structure and chemistry of human serum albumin. *Nature*, **358**, 209–215.
3. Sugio, S., Kashima, A., Mochizuki, S., Noda, M. & Kobayashi, K. (1999). Crystal structure of human serum albumin at 2.5 Å resolution. *Protein Eng.* **12**, 439–446.
4. Kragh-Hansen, U., Chuang, V. T. G. & Otagiri, M. (2002). Practical aspects of the ligand-binding and enzymatic properties of human serum albumin. *Biol. Pharm. Bull.* **25**, 695–704.
5. Spector, A. A. (1986). Structure and lipid binding properties of serum albumin. *Methods Enzymol.* **128**, 320–339.
6. Curry, S., Mandelkow, H., Brick, P. & Franks, N. (1998). Crystal structure of human serum albumin complexed with fatty acid reveals an asymmetric distribution of binding sites. *Nature Struct. Biol.* **5**, 827–835.
7. Curry, S., Brick, P. & Franks, N. P. (1999). Fatty acid binding to human serum albumin: new insights from crystallographic studies. *Biochim. Biophys. Acta*, **1441**, 131–140.
8. Bhattacharya, A. A., Grüne, T. & Curry, S. (2000). Crystallographic analysis reveals common modes of binding of medium and long-chain fatty acids to human serum albumin. *J. Mol. Biol.* **303**, 721–732.
9. Hamilton, J. A., Era, S., Bhamidipati, S. P. & Reed, R. G. (1991). Locations of the three primary binding sites for long-chain fatty acids on bovine serum albumin. *Proc. Natl Acad. Sci. USA*, **88**, 2051–2054.
10. Sudlow, G., Birkett, D. J. & Wade, D. N. (1975). The characterization of two specific drug binding sites on human serum albumin. *Mol. Pharmacol.* **11**, 824–832.
11. Ghuman, J., Zunszain, P. A., Petitpas, I., Bhattacharya, A. A., Otagiri, M. & Curry, S. (2005). Structural basis of the drug-binding specificity of human serum albumin. *J. Mol. Biol.* **353**, 38–52.
12. Kragh-Hansen, U. (1981). Molecular aspects of ligand binding to serum albumin. *Pharmacol. Rev.* **33**, 17–53.
13. Kragh-Hansen, U., Dørge, E. & Pedersen, A. O. (2005). Rate-of-dialysis technique: theoretical and practical aspects. *Anal. Biochem.* **340**, 145–153.
14. Kenyon, M. A. & Hamilton, J. A. (1994). ^{13}C NMR studies of the binding of medium-chain fatty acids to human serum albumin. *J. Lipid Res.* **35**, 458–467.
15. Kragh-Hansen, U. (1991). Octanoate binding to the indole- and benzodiazepine-binding region of human serum albumin. *Biochem. J.* **273**, 641–644.
16. Ashbrook, J. D., Spector, A. A. & Fletcher, J. E. (1972). Medium chain fatty acid binding to human plasma albumin. *J. Biol. Chem.* **247**, 7038–7042.
17. Honoré, B. & Brodersen, R. (1988). Detection of carrier heterogeneity by rate of ligand dialysis: medium-chain fatty acid interaction with human serum albumin and competition with chloride. *Anal. Biochem.* **171**, 55–66.
18. Goodman, D. S. (1958). The interaction of human serum albumin with long-chain fatty acid anions. *J. Am. Chem. Soc.* **80**, 3892–3898.
19. Peyre, V., Lair, V., André, V., le Maire, G., Kragh-Hansen, U., le Maire, M. & Møller, J. V. (2005). Detergent binding as a sensor of hydrophobicity and polar interactions in the binding cavities of proteins. *Langmuir*, **21**, 8865–8875.
20. Pedersen, A. O., Hust, B., Andersen, S., Nielsen, F. & Brodersen, R. (1986). Laurate binding to human serum albumin. Multiple binding equilibria investigated by a dialysis exchange method. *Eur. J. Biochem.* **154**, 545–552.
21. Ashbrook, J. D., Spector, A. A., Santos, E. C. & Fletcher, J. E. (1975). Long chain fatty acid binding to human plasma albumin. *J. Biol. Chem.* **250**, 2333–2338.
22. Oida, T. (1986). ^{1}H-NMR study on the interactions of

human serum albumin with free fatty acid. *J. Biochem.* **100**, 1533–1542.
23. Pedersen, A. O., Honoré, B. & Brodersen, R. (1990). Thermodynamic parameters for binding of fatty acids to human serum albumin. *Eur. J. Biochem.* **190**, 497–502.
24. Pedersen, A. O., Mensberg, K.-L. D. & Kragh-Hansen, U. (1995). Effects of ionic strength and pH on the binding of medium-chain fatty acids to human serum albumin. *Eur. J. Biochem.* **233**, 395–405.
25. Pedersen, A. O. & Brodersen, R. (1988). Myristic acid binding to human serum albumin investigated by dialytic exchange rate. *J. Biol. Chem.* **263**, 10236–10239.
26. Tanford, C. (1972). Hydrophobic free energy, micelle formation and the association of proteins with amphiphiles. *J. Mol. Biol.* **67**, 59–74.
27. Watanabe, H., Tanase, S., Nakajou, K., Maruyama, T., Kragh-Hansen, U. & Otagiri, M. (2000). Role of Arg-410 and Tyr-411 in human serum albumin for ligand binding and esterase-like activity. *Biochem. J.* **349**, 813–819.
28. Watanabe, H., Kragh-Hansen, U., Tanase, S., Nakajou, K., Mitarai, M., Iwao, Y. *et al.* (2001). Conformational stability and warfarin-binding properties of human serum albumin studied by recombinant mutants. *Biochem. J.* **357**, 269–274.
29. Nakajou, K., Watanabe, H., Kragh-Hansen, U., Maruyama, T. & Otagiri, M. (2003). The effect of glycation on the structure, function and biological fate of human serum albumin as revealed by recombinant mutants. *Biochim. Biophys. Acta*, **1623**, 88–97.
30. Fasano, M., Curry, S., Terreno, E., Galliano, M., Fanali, G., Narciso, P. *et al.* (2005). The extraordinary ligand binding properties of human serum albumin. *IUBMB Life*, **57**, 787–796.
31. Yamasaki, K., Maruyama, T., Yoshimoto, K., Tsutsumi, Y., Narazaki, R., Fukuhara, A. *et al.* (1999). Interactive binding to the two principal ligand binding sites of human serum albumin: effect of the neutral-to-base transition. *Biochim. Biophys. Acta*, **1432**, 313–323.
32. Simard, J. R., Zunszain, P. A., Ha, C.-E., Yang, J. S., Bhagavan, N. V., Petitpas, I. *et al.* (2005). Locating high-affinity fatty acid-binding sites on albumin by x-ray crystallography and NMR spectroscopy. *Proc. Natl Acad. Sci. USA*, **102**, 17958–17963.
33. Sjödin, T. (1977). Circular dichroism studies on the inhibiting effect of oleic acid on the binding of diazepam to human serum albumin. *Biochem. Pharmacol.* **26**, 2157–2161.
34. Cunningham, V. J., Hay, L. & Stoner, H. B. (1975). The binding of L-tryptophan to serum albumins in the presence of non-esterified fatty acids. *Biochem. J.* **146**, 653–658.
35. Koh, S.-W. M. & Means, G. E. (1979). Characterization of a small apolar anion binding site of human serum albumin. *Arch. Biochem. Biophys.* **192**, 73–79.
36. Simard, J., Zunszain, P. A., Hamilton, J. A. & Curry, S. (2006). Location of high and low affinity fatty acid binding sites on human serum albumin revealed by NMR drug-competition analysis. *J. Mol. Biol.* **361**, 336–351.
37. Kragh-Hansen, U., Pedersen, A. O., Galliano, M., Minchiotti, L., Brennan, S. O., Tárnoky, A. L. *et al.* (1996). High-affinity binding of laurate to naturally occurring mutants of human serum albumin and proalbumin. *Biochem. J.* **320**, 911–916.
38. Campagnoli, M., Kragh-Hansen, U., Pedersen, A. O., Amoresano, A., Lyon, A. W., Cesati, R. *et al.* (2003). Structural analysis, fatty acid and thyroxine binding properties of Vancouver and Naskapi variants of human serum albumin. *Clin. Biochem.* **36**, 597–605.
39. Chen, R. F. (1967). Removal of fatty acids from serum albumin by charcoal treatment. *J. Biol. Chem.* **242**, 173–181.

Edited by R. Huber

(Received 7 June 2006; received in revised form 17 July 2006; accepted 22 August 2006)
Available online 25 August 2006

0022-3565/07/3203-969–977$20.00
THE JOURNAL OF PHARMACOLOGY AND EXPERIMENTAL THERAPEUTICS
Copyright © 2007 by The American Society for Pharmacology and Experimental Therapeutics
JPET 320:969–977, 2007

Vol. 320, No. 3
114959/3176550
Printed in U.S.A.

S-Nitrosylation of Human Variant Albumin Liprizzi (R410C) Confers Potent Antibacterial and Cytoprotective Properties

Yu Ishima, Tomohiro Sawa, Ulrich Kragh-Hansen, Yoichi Miyamoto, Sadaharu Matsushita, Takaaki Akaike, and Masaki Otagiri

Department of Biopharmaceutics, Graduate School of Pharmaceutical Sciences (Y.I., S.M., M.O.) and Department of Microbiology, Graduate School of Medical Sciences (Y.I., T.S., T.A.), Kumamoto University, Kumamoto, Japan; Department of Medical Biochemistry, University of Aarhus, Aarhus, Denmark (U.K.-H.); and Department of Biochemistry, School of Dentistry, Showa University, Tokyo, Japan (Y.M.)

Received October 3, 2006; accepted November 27, 2006

ABSTRACT

The *S*-nitrosylated forms of certain proteins such as albumin have been thought to be circulating endogenous reservoirs of nitric oxide (NO) and may have potential as NO donors in therapeutic applications. In this study, we investigated the characteristics of R410C, a genetic variant of human serum albumin with two free thiols at positions 34 (Cys-34) and 410 (Cys-410), as a NO carrier via *S*-nitroso formation. A biotin switch assay revealed that Cys-410 was more rapidly and efficiently nitrosylated than was Cys-34. Nitrosylation of Cys-410 introduced only small conformational changes in the protein, which were detected by far-UV circular dichroism but not by near-UV circular dichroism. In addition, both native R410C and *S*-nitrosylated R410C did not induce molecular heterogeneity through oligomerization. *S*-Nitrosylated R410C exhibited strong antibacterial activity against *Salmonella typhimurium* in vitro and suppressed apoptosis of U937 human promonocytic cells induced by Fas ligand. In a rat ischemia-reperfusion liver injury model, *S*-nitrosylated R410C treatment significantly reduced liver damage, as indicated by markedly decreased release of liver enzymes (aspartate aminotransferase and alanine aminotransferase). Pharmacokinetic analyses indicated retention of the *S*-nitroso moiety of *S*-nitrosylated R410C in circulation after i.v. injection, with an approximate half-life of 20.4 min in the mouse. These data suggest that R410C can be a useful NO carrier and can be regarded as a new class of *S*-nitrosylated proteins possessing antibacterial and cytoprotective properties with a circulation time sufficient for in vivo biological activity.

S-Nitrosothiols are nitric oxide (NO) adducts formed endogenously via reaction of thiols with NO or its reactive metabolites such as N_2O_3 and nitrosonium (NO^+)-like species (Akaike, 2000). *S*-Nitrosothiols may function as NO reservoirs and preserve antioxidant properties of NO (Hogg, 2000; Foster et al., 2003). For example, *S*-nitroso human serum albumin (SNO-HSA) has been suggested to serve in vivo as a reservoir for NO produced by endothelial cells (Stamler et al., 1992). In addition, administration of *S*-nitroso albumins to animals with ischemia-reperfusion injury minimized the extent of tissue damage associated with reperfusion. This injury is characterized by initial tissue damage during the ischemic period followed by progressive injury during the reperfusion period. Reperfusion is a trigger for the generation of reactive oxygen species, release of cytokines, induction of adhesion molecules on vascular endothelial cells, and the adhesion and extravasation of leukocytes into postischemic tissue (Hallstrom et al., 2002; Dworschak et al., 2004). Potent cytoprotection against ischemia-reperfusion liver injury in rats (Ikebe et al., 2000) and antibacterial activity in vitro against several types of bacteria (Miyamoto et al., 2000a,b) resulted after human α_1-protease inhibitor (α_1-PI), an acute phase reactive protein in serum, was *S*-nitrosylated (SNO-α_1-PI). These cytoprotective and antibacterial activities of

This work was supported, in part, by grants-in-aid for Scientific Research from the Ministry of Education, Culture, Sports, Science and Technology (MEXT), Japan, and by Fonden af 1870.

Article, publication date, and citation information can be found at http://jpet.aspetjournals.org.

doi:10.1124/jpet.106.114959.

ABBREVIATIONS: NO, nitric oxide; SNO-HSA, *S*-nitroso human serum albumin; α_1-PI, α_1-protease inhibitor; GSNO, *S*-nitrosoglutathione; R410C, genetic variant of human serum albumin mutated at position 410; PAGE, polyacrylamide gel electrophoresis; MMTS, methyl methanethiosulfonate; DTT, 1,4-dithiothreitol; biotin-HPDP, *N*-[6-(biotinamido)hexyl]-3′-(2′-pyridyldithio) propionamide; p-NONOate, propylamine NONOate; CNBr, cyanogen bromide; SH, thiol; DTPA, diethylenetriaminepentaacetic acid; CBB, Coomassie Brilliant Blue; HPLC, high-performance liquid chromatography; CD, circular dichroism; HENS, 250 mM HEPES buffer (pH 7.7) containing 1 mM EDTA, 0.1 mM neocuproine, and 1% SDS; FITC, fluorescein isothiocyanate; ALT, alanine aminotransferase; AST, aspartate aminotransferase; AUC, area under the plasma concentration-time curve; FasL, Fas ligand.

SNO-α_1-PI were more powerful than those of NO alone and of low-molecular-weight *S*-nitrosothiols such as *S*-nitrosoglutathione (GSNO) (Miyamoto et al., 2000a,b). In addition to serving as a reservoir for NO, *S*-nitrosothiols themselves have been suggested to show various biological activities, possibly through transnitrosylation, *S*-thiolation, and direct action of other biological molecules (Hogg, 2000; Miyamoto et al., 2000a; Foster et al., 2003). These observations suggest many potential clinical uses for *S*-nitrosothiols, not only as NO-releasing agents but also as members of a new class of therapeutic agents (Richardson and Benjamin, 2002).

Researchers in several laboratories have investigated genetic variants of HSA to define the functional defects and correlate them with molecular and biochemical properties and stability of the molecules. So far, approximately 60 amino acid substitutions have been characterized (Kragh-Hansen et al., 2004). Among them, albumin Liprizzi (R410C) represents the only instance of a mutation located in the hydrophobic binding pocket of subdomain IIIA (Galliano et al., 1998). The amino acid substitution of the variant introduces an additional cysteine residue (Cys-410), which is far from disulfide bonds and from the normal Cys-34. Therefore, the presence of the new cysteine residue does not alter the disulfide pattern or cause gross conformational changes in the protein (Galliano et al., 1998). These observations led us to hypothesize that Cys-410 might be a target of *S*-nitrosylation, and if so, multiple *S*-nitroso sites might be introduced in a single HSA molecule to prepare a new SNO-HSA formulation.

In the present study, we investigated the kinetics of *S*-nitrosylation of Cys-34 and Cys-410 in R410C by means of a biotin switch assay. Effects of *S*-nitrosylation on structural stability of the proteins were examined by using UV spectroscopy and nonreducing SDS-polyacrylamide gel electrophoresis (PAGE). Antibacterial and antiapoptotic activities of the synthesized SNO-R410C were studied in vitro and compared with those of high- and low-molecular-weight *S*-nitrosothiols, including SNO-HSA, SNO-α_1-PI, GSNO, and non-*S*-nitrosothiol types of NO donors. We also examined the cytoprotective capability of SNO-R410C in an ischemia-reperfusion liver injury model in rats. Finally, we determined the pharmacokinetic parameters of the *S*-nitrosylated proteins in mice.

Materials and Methods

Materials. Sephadex G-25 (ϕ 1.6 × 2.5 cm), Blue Sepharose CL-6B (ϕ 2.5 × 20 cm), and RESOURCE PHE (ϕ 0.64 × 3 cm) were from GE Healthcare (Tokyo, Japan). Enzymes for DNA assays were from Takara (Kyoto, Japan). The *Pichia* Expression kit was from Invitrogen (Carlsbad, CA). Methyl methanethiosulfonate (MMTS), neocuproine, ascorbic acid, 1,4-dithiothreitol (DTT), and glutathione were purchased from Sigma-Aldrich (St. Louis, MO). *N*-[6-(Biotinamido)hexyl]-3′-(2′-pyridyldithio) propionamide (biotin-HPDP) was obtained from Pierce (Rockford, IL). Sulfanilamide, naphthylethylenediamine hydrochloride, $HgCl_2$, $NaNO_2$, $NaNO_3$, and CNBr were obtained from Nakalai Tesque (Kyoto, Japan). Isoamyl nitrite was purchased from Wako Chemicals (Osaka, Japan). GSNO, propylamine NONOate (p-NONOate), 5,5′-dithiobis-2-nitrobenzoic acid, diethylenetriaminepentaacetic acid (DTPA), and EDTA were obtained from Dojindo Laboratories (Kumamoto, Japan). $^{111}InCl_3$ (74 MBq/ml in 0.02 N HCl) was a gift from Nihon Medi-Physics Co., Ltd. (Hyogo, Japan). Other chemicals were of the best grades commercially available.

Nonrecombinant Proteins. The HSA preparation consisting of different ratios of native HSA and R410C (Galliano et al., 1998) were provided by Drs. M. Galliano and L. Minchiotti (University of Pavia, Italy). The samples were defatted by treatment with a hydroxyalkoxypropyl dextran at pH 3.0 (Kragh-Hansen, 1993). nHSA was donated by the Chemo-Sera-Therapeutic Research Institute (Kumamoto, Japan) and was defatted by treatment with charcoal as described by Chen (1967).

Generation of *Pichia pastoris* Producing HSA and the R410C Mutant. The expression vector pPIC9-wHSA containing the native HSA expression cassette stably integrated into the chromosomal DNA was used to produce HSA (Matsushita et al., 2004). We made the R410C mutant by using the QuikChange XL site-directed mutagenesis kit (Stratagene, La Jolla, CA), with the following mutagenic primers (sense and antisense): 5′-GAATGCGCTATTAGTTTGCTACACCAAGAAAGTACCC-3′ and 3′-GGGTACTTTCTTGGTGTAGCAAACTAATAGCGCATTC-5′.

The constructed plasmids (pPIC9-wHSA and pPIC9-HSA R410C) were transferred to XL10-Gold *Escherichia coli* organisms, which were grown in Luria-Bertani medium. After plasmid purification from *E. coli*, the plasmid sequences were confirmed by use of the dideoxy chain termination method with a PerkinElmer (Boston, MA) ABI Prism 310 Genetic Analyzer. *P. pastoris* GS115 *his4* was transformed with SalI-digested pPIC9-wHSA or pPIC9-HSA R410C by electroporation according to the manual (EasySelect *Pichia* Expression Kit Version A; Invitrogen). Histidine-independent transformants were selected and subsequently screened for slow methanol utilization phenotypes. Positive clones were induced with methanol and screened for production of HSA or R410C mutants by 12.5% SDS-PAGE of culture medium.

Production and Purification of Recombinant Albumins. The protocol used to express the HSA was a modification of a previously published protocol (Matsushita et al., 2004). Single colonies of *P. pastoris* were grown (30°C, 210 rpm, 48 h) in 300 ml of BMGY growth medium (1% yeast extract, 2% peptone, 100 mM potassium phosphate, pH 6.0, 1.34% yeast nitrogen base, 4×10^{-5}% biotin, and 1% glycerol) in 1-liter baffled flasks until an A_{600} value of 2 to 6 was obtained. Cells were then harvested by centrifugation at 3000*g*, and cell pellets were washed extensively and resuspended in 300 ml of BMMY medium (1% yeast extract, 2% peptone, 100 mM potassium phosphate, pH 6.0, 1.34% yeast nitrogen base, 4×10^{-5}% biotin, and 1% methanol) to an approximate A_{600} value of 15 to 20. For further culture of this *P. pastoris* suspension, the baffled flasks were shaken (30°C, 190 rpm, 96 h) with daily addition (every 12 h) of methanol at a final concentration of 1% to maintain the induction conditions of the alcohol oxidase 1 promoter.

The recombinant proteins were purified after 96 h of induction, according to the literature (Matsushita et al., 2004). The protein preparation was first subjected to chromatography with the Blue Sepharose CL-6B column (ϕ 2.5 × 20 cm) equilibrated with 50 mM sodium phosphate buffer (pH 7.0) after dialysis with the same buffer. Proteins were further purified by using the RESOURCE PHE column (ϕ 0.64 × 3.0 cm) equilibrated with 50 mM sodium phosphate buffer, pH 7.0, containing 1.5 M ammonium sulfate. The column was washed with the phosphate buffer and then eluted with a 20-ml gradient of ammonium sulfate, 1.5 to 0 M, in the same buffer. The eluted HSA were deionized and defatted via charcoal treatment, freeze-dried, and then stored at −20°C until used. Sample purity was estimated by density analysis of Coomassie Brilliant Blue (CBB)-stained protein bands on 12.5% SDS-PAGE. The recombinant protein samples of HSA and R410C were judged as more than 97% pure.

***S*-Nitrosylation of the Proteins.** *S*-Nitrosylated proteins were prepared according to previous reports (Akaike et al., 1997; Ikebe et al., 2000). In brief, protein (300 μM) was incubated with DTT (molar ratio, protein/DTT = 1:10) for 5 min at 37°C. DTT was then quickly removed by Sephadex G-25 gel filtration and eluted with 0.1 M potassium phosphate buffer (pH 7.4) containing 0.5 mM DTPA. Samples of DTT-treated proteins (0.1 mM) were incubated with

isoamyl nitrite (molar ratio, protein/isoamyl nitrite = 1:10) in 0.1 M potassium phosphate buffer (pH 7.4) containing 0.5 mM DTPA for 60 min at 37°C. *S*-Nitrosylated products were purified by Sephadex G-25 gel filtration, eluted with pure water, and concentrated by ultrafiltration (cutoff size of 7500 Da). These samples were stored at −80°C until use. The protein content of all the protein preparations used in this study was determined by the Bradford assay.

Determination of *S*-Nitrosylation Efficiency. The amounts of the *S*-nitroso moiety of SNO-HSA, SNO-R410C, and SNO-α_1-PI were quantified by high-performance liquid chromatography (HPLC) coupled with a flow reactor system, as previously reported (Akaike et al., 1997). The stability of the *S*-nitroso moiety on storage in neutral solution was examined as follows. The modified proteins were dissolved in 100 mM potassium phosphate buffer containing 0.5 mM DTPA (pH 7.4) and left in the dark at room temperature for a maximum of 21 days. At appropriate times after the start of incubation, aliquots of the *S*-nitrosylated protein solutions were taken and injected into the HPLC flow reactor system to detect *S*-nitrosylated compounds. The effect of lyophilization was studied by redissolving lyophilized samples in 100 mM potassium phosphate buffer containing 0.5 mM DTPA (pH 7.4). *S*-Nitroso moieties of the *S*-nitrosylated proteins were quantified before and after the redissolving.

Physicochemical Characterization of the *S*-Nitrosylated Albumins. Gross conformational changes induced by *S*-nitrosylation of recombinant HSA were assessed by means of nonreducing SDS-PAGE at 4°C in the dark, with use of a standard curve prepared with a set of marker proteins (Full Range Rainbow Marker; GE Healthcare, Tokyo, Japan). Circular dichroism (CD) spectra of HSA, R410C, and their *S*-nitrosylated products were measured at 25°C using a J-720-type spectropolarimeter (JASCO, Tokyo, Japan). For calculation of mean residue ellipticity [θ], the molecular weight of the albumins was taken as 66,500. Far-UV and near-UV CD spectra were recorded at protein concentrations of 5 and 15 μM, respectively, in 20 mM sodium phosphate buffer (pH 7.4).

To determine the sites and kinetics of *S*-nitrosylation, the biotin switch assay was performed, as reported earlier (Jaffrey et al., 2001). Specifically, HSA or R410C (0.3 mM) was incubated with GSNO (1.5 mM) in 100 mM potassium phosphate buffer (pH 7.8) for 5 or 60 min at 37°C. After the incubation, the reaction mixture was immediately applied to a G-25 gel filtration column eluted with HENS buffer (250 mM HEPES, pH 7.7, 1 mM EDTA, 0.1 mM neocuproine, and 1% SDS) to terminate the reaction. Fractions containing protein were collected and combined. Protein concentrations were adjusted to be 0.5 mg/ml, followed by treatment with MMTS to block free SH. To block free SH groups on the protein without affecting the disulfide bonds, 4 volumes of blocking buffer (225 mM HEPES, pH 7.7, 0.9 mM EDTA, 0.09 mM neocuproine, 2.5% SDS, and 20 mM MMTS) were added. The resulting solutions were agitated for 20 min at 50°C. Proteins were then recovered by precipitation with acetone (final concentration, 50%), and the precipitates were resuspended in 0.1 ml of HENS buffer (protein concentration, 10 mg/ml). To this protein solution was added 0.1 ml of biotin-HPDP (4 mM) in *N,N*-dimethylformamide and 0.1 ml of aqueous ascorbate (0 or 1 mM), and the samples were incubated for 1 h at room temperature. Proteins were then recovered via acetone precipitation. The biotinylated proteins were dissolved in 0.1 ml of 70% formic acid containing 0.64 mg of CNBr (CNBr/methionine residues = 200:1), and samples were incubated under N_2 for 24 h in the dark at room temperature. An aliquot of 1 ml of Milli-Q water was added at the end of the CNBr cleavage to stop the reaction, and the resulting mixture was lyophilized. Lyophilized fragments were resuspended in 0.05 ml of Milli-Q water. The mixture of fragments was separated on 10 to 20% gradient SDS-PAGE gel. The fragment size was determined by use of a calibration curve obtained from size markers, and each fragment was assigned according to its molecular size. To analyze biotinylated fragments, samples prepared as above were separated on 10 to 20% gradient SDS-PAGE gels, transferred to polyvinylidene fluoride membranes (Immobilon-P; Millipore Corporation, Bedford, MA), blocked with 3% bovine serum albumin, and incubated with streptavidin-horseradish peroxidase diluted 1/2000 for 40 min.

Antibacterial Activity of *S*-Nitrosothiols. In vitro antibacterial activities of various *S*-nitrosothiols and a non-*S*-nitrosothiol-type NO donor (p-NONOate) were examined according to previously reported methods, with slight modification (Miyamoto et al., 2000a). We used M9 medium (pH 7.4) during incubation of bacteria with *S*-nitrosothiols and the NO donor. In brief, *Salmonella typhimurium* LT2 organisms were cultured overnight in M9 medium and were then washed three times with M9 medium. The bacteria were resuspended in Krebs-Ringer phosphate buffer containing 1 mg/ml NH_4Cl and 5 mg/ml thiamine hydrochloride. The bacterial suspension (1×10^6 CFU/ml, 0.02 ml in M9 medium) was mixed with 0.18 ml of M9 medium containing various concentrations of *S*-nitrosothiols or p-NONOate in a 96-well plate. After 1 h of incubation at 37°C, the bacteria were collected by centrifugation (1500*g*, 5 min), resuspended in 0.18 ml of M9 medium, transferred to another 96-well plate, and incubated for 9 h at 37°C. The numbers of bacteria exposed to various *S*-nitrosothiols were determined by measuring the turbidity of the culture suspension. A_{655} value was monitored by using a microplate reader (model 450; Bio-Rad Laboratories, Hercules, CA).

Effect of *S*-Nitrosothiols on Apoptosis. U937 human promonocytic cells were grown in Dulbecco's modified Eagle's medium that was supplemented with 10% fetal bovine serum and 1% penicillin-streptomycin. The cells were maintained in a humidified incubator (95% air, 5% CO_2) at 37°C. Cells from this culture (5×10^5 cells/ml) were treated with *S*-nitrosothiols for 6 h in the dark and were then washed with phosphate-buffered saline three times to remove the *S*-nitrosothiols. After this washing, cells were reacted with 200 ng/ml anti-Fas antibody (Medical and Biological Laboratories, Nagoya, Japan). After 9 h of incubation, the number of apoptotic cells was determined with an annexin V-fluorescein isothiocyanate (FITC) binding assay kit from BD Biosciences (Tokyo, Japan). The fluorescence of annexin V-FITC and propidium iodide was measured via a FACSCalibur flow cytometer (BD Biosciences), using the FL1 and FL2 channels, respectively.

Cytoprotective Effect of SNO-HSA in Vivo. A rat ischemia-reperfusion liver injury model served for investigation of the cytoprotective effect of *S*-nitrosothiols, according to a previous report (Ikebe et al., 2000). Male Wistar rats weighing between 200 and 230 g (Kyudo, Inc., Kumamoto, Japan) were used. The animals were fasted for 9 h before surgery but were allowed access to water. The rats were anesthetized with ether during the operation. After the abdomen was shaved and disinfected with 70% ethanol, a complete midline incision was made. The portal vein and hepatic artery were exposed and cross-clamped for 30 min with a noncrushing microvascular clip. Saline, as the vehicle control, or various compounds including HSA, R410C, SNO-HSA, and SNO-R410C (usually 0.1 μmol/rat) were given via the portal vein immediately after reperfusion was initiated. The abdomen then was closed in two layers with 2-0 silk. The rats were kept under warming lamps until they awakened and became active.

Because blood loss caused by frequent blood sampling could affect liver functions, animals were sacrificed by taking whole circulating blood via abdominal aorta under anesthesia at various time points after reperfusion was initiated. Plasma alanine aminotransferase (ALT) and aspartate aminotransferase (AST) activities were measured by using a sequential multiple AutoAnalyzer system from Wako Chemicals, with activities expressed in international units per liter. All the animal experiments were carried out according to the guidelines of the Laboratory Protocol of Animal Handling, Graduate School of Medical Sciences, Kumamoto University.

Pharmacokinetic Experiments. Proteins were labeled with ^{111}In by using DTPA anhydride as a bifunctional chelating agent (Hnatowich et al., 1982; Yamasaki et al., 2002). Labeled proteins were injected via the tail vein into male ddY mice (weighing 25–27 g) at a dose of 0.1 mg/kg. At appropriate times after injection, blood was

collected from the vena cava with the mouse under ether anesthesia. Heparin sulfate was used as an anticoagulant, and plasma was obtained from the blood by centrifugation. Liver, kidneys, spleen, heart, and muscle samples were obtained, rinsed with saline, and weighed. The radioactivity in each sample was counted using a well-type NaI scintillation counter ARC-2000 (Aloka, Tokyo, Japan). ^{111}In radioactivity concentrations in plasma were normalized as a percentage of the dose per milliliter and were analyzed by means of the nonlinear least-squares program MULTI (Yamaoka et al., 1981). Tissue distribution profiles were evaluated by using tissue uptake clearance (CL_{tissue}) according to integration plot analysis. By dividing the amount in a tissue at time t (X_t) and the area under the plasma concentration-time curve (AUC) from time 0 to t (AUC_{0-t}) by the plasma concentration at time t (C_t), CL_{tissue} was obtained from the slope of the plot of X_t/C_t versus AUC_{0-t}/C_t. In addition, we measured *S*-nitroso moieties in plasma by means of the Saville assay (Akaike et al., 1997). Similar experiments were performed with nonlabeled GSNO. For that purpose, plasma samples were collected into tubes containing DTPA (final concentration, 2 mM) and centrifuged for 5 min at 1500*g* in the dark. Plasma samples then were analyzed for NO_2^- by means of the Griess reaction.

Statistical Analysis. Analysis of variance followed by the Newman-Keuls method for more than 2 means were used to evaluate the statistical significance of collected data. Data were expressed as mean ± S.E.M. Differences between groups were evaluated by Student's *t* test, and $p < 0.05$ was regarded as statistically significant.

Results

Production of Recombinant R410C. Because the genetic variant cannot be separated from its normal endogenous counterpart, recombinant R410C was generated, via the *P. pastoris* recombinant system, to be used as a pure R410C preparation. After purification by means of column chromatography, 360 mg of R410C with a purity of >97% was obtained from a 3.6-liter culture. SDS-PAGE under nonreducing conditions revealed only a single band for recombinant R410C with a molecular mass of approximately 67 kDa, which indicated successful generation of a homogeneous monomer protein.

Physicochemical Properties of *S*-Nitrosylated R410C (SNO-R410C). We first examined the efficiency of *S*-nitrosylation of HSA by using isoamyl nitrite as the nitrosating agent. The *S*-nitroso moiety of native HSA was determined to be approximately 0.3 mol/mol HSA under the current conditions. When we treated serum-derived HSA containing different proportions of R410C, the *S*-nitroso content increased linearly according to the increasing content of R410C (Fig. 1). The *S*-nitroso content reached 1.3 mol/mol protein for recombinant R410C (R410C/total HSA = 1.0). The difference in *S*-nitroso content between native HSA and R410C was almost 1 mol, which suggests that almost all the Cys-410 residues in R410C may be *S*-nitrosylated.

To study the relative efficiency of *S*-nitrosylation at Cys-34 versus that at Cys-410, *S*-nitrosylation sites were determined by means of the biotin switch assay. Figure 2A shows that CBB staining revealed almost equal amounts of fragments after CNBr treatment of HSA, which confirmed that CNBr protein fragmentation was not affected by *S*-nitrosylation. The biotin switch assay involves three major steps: blockage of free thiols, specific reduction of *S*-nitrosothiols to thiols by ascorbate, and labeling the nascent thiols with biotin groups (Jaffrey et al., 2001). The biotin switch assay (Fig. 2A) clearly found fragment 299 to 585, which contains

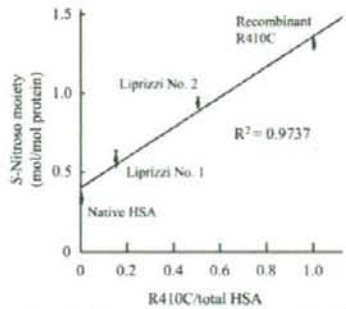

Fig. 1. Efficiency of *S*-nitrosylation of HSA by isoamyl nitrite as a function of R410C content. HSA containing various proportions of R410C was reacted with isoamyl nitrite. The value of the *S*-nitroso moiety was determined by the Griess assay with an HPLC flow reactor system. Data are expressed as mean ± S.E.M. (n = 4–6).

Cys-410, after just 5 min of incubation with GSNO. After 60 min of incubation, fragment 1 to 298, which contains Cys-34, was also detected. To confirm the specificity of the assay, we omitted ascorbate treatment of the protein. As shown in Fig. 2A, no bands were detected for proteins without ascorbate treatment. The time profile of *S*-nitrosylation as quantified by the biotin switch assay indicated that Cys-410 was *S*-nitrosylated more rapidly and efficiently than was Cys-34 (Fig. 2B). Similar results were obtained for *S*-nitrosylation of R410C with use of isoamyl nitrite instead of GSNO (data not shown).

The effect of *S*-nitrosylation on gross conformation was examined by means of nonreducing SDS-PAGE analysis (Fig. 3A). *S*-Nitrosylation caused no dimerization via disulfide bond formation, fragmentation, or other gross conformational changes. Potential conformational alterations were investigated in more detail by means of CD spectrometric analyses (Fig. 3, B–E). According to the far-UV spectra, *S*-nitrosylation of Cys-34 had no detectable effect on the secondary structure of native HSA (Fig. 3B). *S*-Nitrosylation of both Cys-34 and Cys-410 resulted in a small decrease in the α-helical content of the protein (Fig. 3D). In addition, nitrosylation of the cysteine residues had only a small influence, if any, on the tertiary structure of the protein, as evidenced by UV spectra analyses (Fig. 3, C and E). Thus, our data suggest that R410C was structurally stable in aqueous media and that *S*-nitrosylation induced no significant conformational changes.

In addition, we examined the stability of *S*-nitroso moieties in neutral buffer and during lyophilization (data not shown). The half-life of the *S*-nitroso moiety of SNO-R410C was 23.5 days in phosphate buffer, pH 7.4, in the dark. This half-life provided evidence of a fairly stable compound compared with SNO-α_1-PI, which is a stable *S*-nitrosylated protein (18.9 days). Only a slight decrease (~10%) in *S*-nitroso content was observed after lyophilization of SNO-R410C.

Antibacterial Activity of SNO-R410C. NO and related species including *S*-nitrosothiols reportedly inhibit the growth of a wide variety of microorganisms, including viruses, bacteria, parasites, and fungi (Fang, 2004). Miyamoto et al. (2000b) showed that SNO-α_1-PI has a strong bacteriostatic effect against both Gram-negative and Gram-positive bacteria, with the IC_{50} in the low micromolar range. In agreement with previous reports, we found that low-molecular-

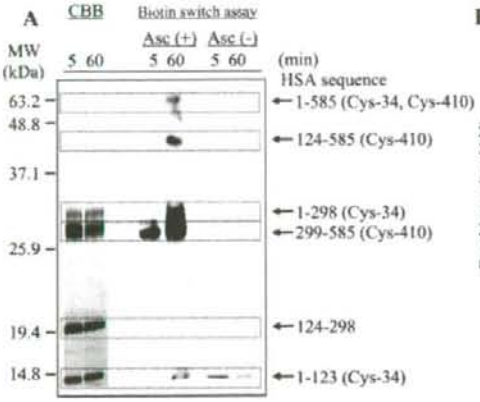

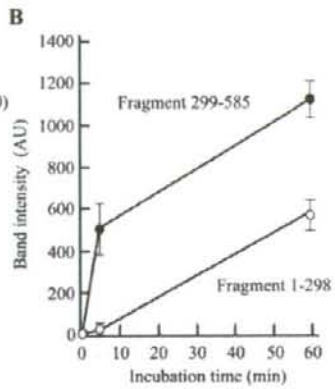

Fig. 2. Analyses of site and rate of *S*-nitrosylation in R410C produced by GSNO. A, SDS-PAGE of R410C cleaved with CNBr, followed by CBB staining or the biotin switch assay with streptavidin-conjugated horseradish peroxidase. B, time profile of *S*-nitrosylation of R410C as determined by the biotin switch assay. Band intensities of fragment 1 to 298 and fragment 299 to 585 were plotted against time of incubation with GSNO. Data are expressed as mean ± S.E.M. (n = 3).

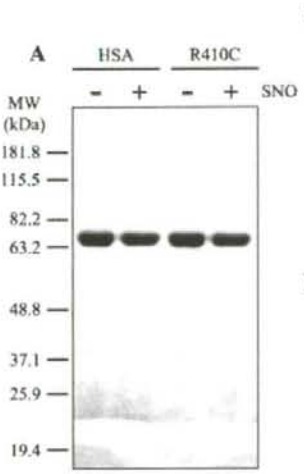

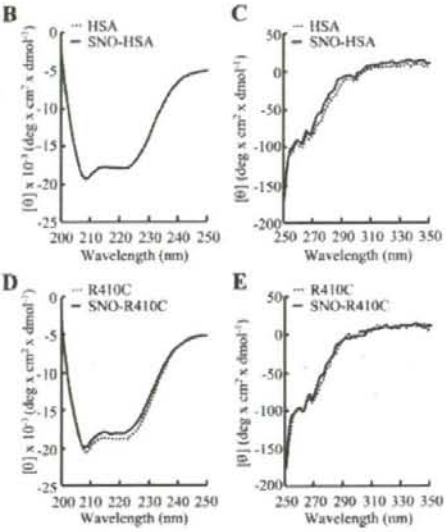

Fig. 3. Structural integrity of HSA and R410C with and without *S*-nitrosylation. A, nonreducing SDS-PAGE, for examination of oligomerization. The gel was stained by CBB. Molecular mass markers are indicated at the left of the gel. B–E, far-UV (B and D) and near-UV (C and E) CD spectra for HSA (B and C) and R410C (D and E) with and without *S*-nitrosylation.

weight NO donors such as GSNO and p-NONOate had a very weak antibacterial effect, with an IC_{50} value of approximately 3 mM (Fig. 4). SNO-α_1-PI, used as a positive control, suppressed bacterial growth with an IC_{50} value of approximately 6 μM. SNO-HSA was as potent as SNO-α_1-PI, with an IC_{50} value of approximately 8 μM, in suppressing bacterial growth. The corresponding value for SNO-R410C was submicromolar (0.6 μM), which indicated that the antibacterial activity of SNO-R410C was 10 and 13 times stronger than that of SNO-α_1-PI and SNO-HSA, respectively. Parental R410C had no antibacterial activity (data not shown).

Effect of SNO-R410C on Apoptosis of Cells Induced by Fas Ligand. NO and related species reportedly induce both antiapoptotic and proapoptotic responses in cells, the type of response depending on the concentrations of the NO donors, cell types, and apoptosis-inducing reagents (Kim et al., 1999). In the present study, we examined the effect of SNO-R410C on apoptosis of U937 cells induced by Fas ligand (FasL). Under the present experimental conditions, 65% of the total number of cells underwent apoptotic cell death after

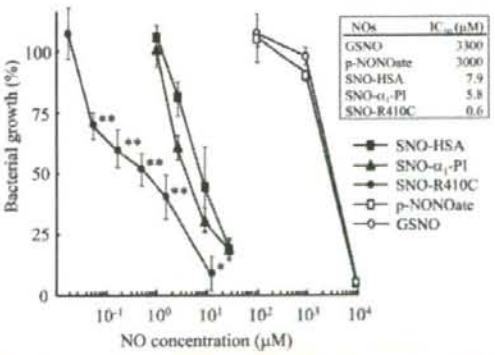

Fig. 4. Concentration-dependent antibacterial effects of *S*-nitrosothiols and p-NONOate. Bacterial growth, assessed by means of turbidity and expressed as a percentage of control, was determined at 12 h after incubation with or without various compounds. Data are expressed as mean ± S.E.M. (n = 3–6). *, $p < 0.05$ and **, $p < 0.01$ compared with SNO-α_1-PI.

treatment with FasL (Fig. 5). This apoptotic change was significantly suppressed by SNO-R410C; however, the other *S*-nitrosylated compounds—SNO-HSA and GSNO—showed only a marginal inhibitory effect.

Cytoprotective Effect of SNO-R410C against Ischemia-Reperfusion Liver Injury in Rats. We used an ischemia-reperfusion liver injury model in rats (Ikebe et al., 2000) to examine the cytoprotective effect of SNO-R410C. Previous studies with SNO-α_1-PI showed that a quantity of 0.1 μmol/rat was most suitable for this kind of experiment (Ikebe et al., 2000). Therefore, we used the same quantity of SNO-R410C. However, the effect was dose-dependent, but even a dose of 0.01 μmol/rat had a cytoprotective effect (data not shown). To evaluate liver injury, we measured the extracellular release of the liver enzymes AST and ALT via plasma enzyme values. As reported previously for SNO-α_1-PI and α_1-PI (Ikebe et al., 2000), these values increased to a maximum at 2 h after reperfusion and then decreased gradually during 24 h (data not shown). Native HSA and R410C did not modify liver damage in this model (Fig. 6). However, a significant reduction in release of AST and ALT was observed in rats treated with SNO-R410C, with this reduction also significantly greater than that noted for SNO-HSA. Even at 12 h after reperfusion, the levels of AST and ALT remained significantly lower in SNO-R410C-treated animals than in control animals, although the difference was not so great compared with that observed at 2 h after reperfusion (data not shown). At 24 h after reperfusion, no significant difference in the levels of AST and ALT was observed between SNO-R410C-treated animals and control animals because the liver damage in both groups was almost recovered to the basal level (data not shown).

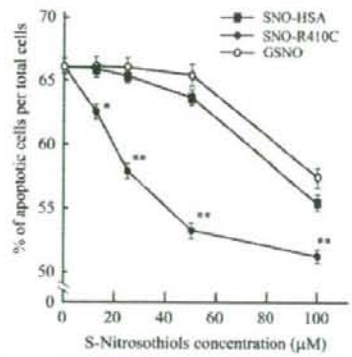

Fig. 5. Antiapoptotic effects of *S*-nitrosothiols. U937 cells were treated with anti-Fas antibody to induce apoptotic cell death. Numbers of dead cells were determined by means of flow cytometry with annexin V-FITC and propidium iodide. SNO-HSA, SNO-R410C, and GSNO were added to cell cultures at the indicated concentrations. Data are expressed as mean ± S.E.M. (n = 5–9). *, $p < 0.05$ and **, $p < 0.01$ compared with SNO-HSA.

Pharmacological Properties of SNO-R410C. We determined pharmacokinetic characteristics of HSA, R410C, and their *S*-nitrosylated counterparts in mice. Figure 7A indicates that the plasma concentration of R410C decreased more rapidly than did that of HSA. *S*-Nitrosylation of R410C slightly prolonged the plasma half-life of R410C (Fig. 7A). Kidney uptake of R410C (Fig. 7C) was not affected by *S*-nitrosylation, whereas liver uptake of R410C (Fig. 7D) was significantly suppressed after *S*-nitrosylation. As shown in Table 1, R410C had higher clearance rates than did HSA in both liver and kidney, which may explain the more rapid clearance of R410C from circulation compared with clearance of HSA. Despite this relatively higher clearance rate, the decrease in the *S*-nitroso moiety was only slightly faster for SNO-R410C than for SNO-HSA. Consequently, the *S*-nitroso content per carrier (*S*-NO/carrier) remained appreciably higher for SNO-R410C compared with SNO-HSA, as shown in Table 1. These data suggest that the stability of SNO-R410C is higher than that of SNO-HSA in the circulation. No tissue-specific accumulation of R410C and HSA was observed (data not shown). The plasma *S*-nitroso level became undetectable at 10 min after i.v. injection of GSNO (Fig. 7B). However, even at 120 min after administration, appreciable levels of the *S*-nitroso moieties were detected in plasma of mice receiving SNO-R410C and SNO-HSA (Fig. 7B). The apparent half-lives of the *S*-nitroso moieties were 4.2, 20.4, and 46.3 min for GSNO, SNO-R410C, and SNO-HSA, respectively.

Discussion

NO is a powerful biological agent (Moncada and Higgs, 1993; Liu and Stamler, 1999), but its short in vivo half-life (~0.1 s) sometimes limits its potential biological usefulness.

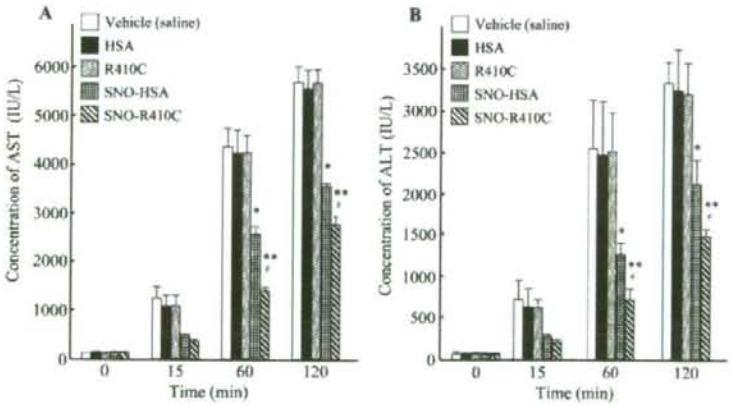

Fig. 6. Time profile of changes in serum levels of AST (A) and ALT (B) after hepatic ischemia-reperfusion in rats. Ischemia was induced by occluding both portal vein and hepatic artery for 30 min, followed by reperfusion. Vehicle (saline), HSA, R410C, SNO-HSA, and SNO-R410C were administered via the portal vein immediately after initiation of reperfusion. Data are expressed as mean ± S.E.M. (n = 4–6 at each time point). *, $p < 0.05$ and **, $p < 0.01$ compared with the vehicle-treated group. #, $p < 0.05$ compared with the SNO-HSA-treated group.

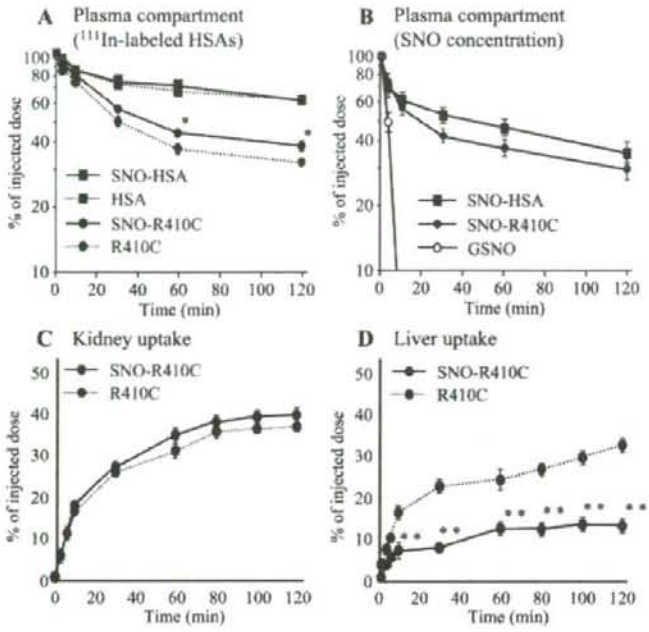

Fig. 7. Plasma concentrations of ^{111}In radioactivity (A) and *S*-nitroso moieties (B) and tissue accumulation of radioactivity in kidney (C) and liver (D) after i.v. injection of HSA, R410C, their *S*-nitrosylated counterparts, or GSNO. *, $p < 0.05$ compared with R410C and **, $p < 0.01$ compared with R410C.

TABLE 1
Uptake clearances and plasma concentration of protein and *S*-nitroso moieties at 120 min after injection of *S*-nitrosylated and native proteins

	Uptake Clearance		Plasma Concentration after 120 Min		
	Liver	Kidney	Carrier	*S*-NO	*S*-NO/Carrier
	ml/h		*% of injected dose*		
HSA					
NO (−)	222 ± 20[a]	48 ± 18	62.6 ± 4.4		
NO (+)	168 ± 14	126 ± 14	63.4 ± 7.2	34.6 ± 8.0	54.6 ± 4.2
R410C					
NO (−)	324 ± 12	408 ± 17	36.2 ± 4.0		
NO (+)	150 ± 13	444 ± 25	42.2 ± 4.7	29.3 ± 5.5	69.4 ± 5.3

[a] Results are expressed as mean ± S.E.M. ($n = 3$).

However, the half-life can be greatly prolonged by forming *S*-nitrosothiols with cysteine residues of proteins, so that, for example, plasma may contain a long-lasting, circulating reservoir. In the present study, we investigated *S*-nitrosylation of R410C, a genetic variant of HSA possessing an additional free cysteine at position 410, and examined the physicochemical, biological, and pharmacokinetic properties of the resultant SNO-R410C. The biotin switch assay revealed that Cys-410 was more rapidly and efficiently *S*-nitrosylated than was Cys-34 in R410C (Fig. 2B), with the *S*-nitroso content increased from 0.3 mol/mol normal HSA to 1.3 mol/mol R410C. Earlier structural analysis (Carter and Ho, 1994; Sugio et al., 1999) reported that Cys-34 is located in a crevice on the surface of the albumin molecule but seems to be surrounded and protected by several other residues. In contrast, Cys-410 lies in a tunnel region in subdomain IIIA and seems to be freely accessible to the extracellular milieu (Bhattacharya et al., 2000). This molecular environment of the Cys-410 residue in R410C is indeed thought to be favorable for *S*-nitrosylation. As illustrated in Fig. 8, Cys-410 is surrounded by acidic (Glu) and basic (Lys) residues, which may constitute the acid-base motif that may facilitate deprotonation of thiol to form a nucleophilic thiyl anion ($-S^-$), as suggested recently by Hess et al. (2005). In addition, the presence of hydrophobic moieties (Tyr) near Cys-410 may stabilize NO and thereby promote formation of N_2O_3, a strong *S*-nitrosylating agent,

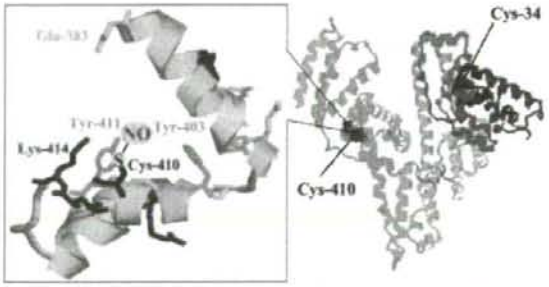

Fig. 8. Proposed locations of Cys-34 and Cys-410 in R410C. The molecular structure was simulated based on X-ray crystallographic data with the use of the RasMol program (http://www.openrasmol.org).

via reaction with molecular oxygen. Together, these factors should thus contribute to effective *S*-nitrosylation of R410C at Cys-410.

Earlier work showed that introduction of multiple *S*-nitroso residues in albumins led to formation of aggregates through intermolecular disulfide formation (Marks et al., 1995; Ewing et al., 1997). Aggregate formation results in induction of molecular heterogeneity, which limits the therapeutic application of *S*-nitroso albumins that have multiple *S*-nitroso residues. Katsumi et al. (2005) reported that conjugation of the water-soluble synthetic polymer polyethylene glycol to albumins with multiple *S*-nitroso residues prevented molecular aggregate formation (Katsumi et al., 2005). In the present study, we found that *S*-nitrosylation did not induce molecular aggregation of R410C, as shown by nonreducing SDS-PAGE analysis (Fig. 3A). Furthermore, CD spectroscopy showed that *S*-nitrosylation had only a small influence on the tertiary structure of the protein (Fig. 3, B–E). These results suggest that multiple *S*-nitroso sites can be introduced in R410C without causing any major conformational changes. It is also important to note that no apparent clinical disorders were observed in human subjects with R410C alloalbuminemia (Galliano et al., 1998). Therefore, we expect SNO-410C to be clinically applicable as a biocompatible pharmacological agent, although further study is required to clarify other issues, including antigenicity of this variant protein.

Our investigation confirmed that *S*-nitrosylation added new biological functions to R410C that were not observed with parental R410C. For example, the present in vitro study with *Salmonella* revealed that SNO-R410C possessed the strongest antibacterial activity among various *S*-nitrosothiols that we have tested (Miyamoto et al., 2000a). Our previous data also showed that transnitrosylation from SNO-α_1-PI to bacteria is a critical step for the antibacterial action of SNO-α_1-PI (Miyamoto et al., 2000a). In addition, the NO-releasing agent p-NONOate had very weak antibacterial activity (Fig. 4). These results suggest that, for its antibacterial function, SNO-R410C may act as a nitroso donor rather than a pure NO donor. Likewise, SNO-R410C was the most potent *S*-nitrosothiol in terms of antiapoptotic activity in FasL-induced apoptosis of U937 cells (Fig. 5).

Reperfusion of ischemic tissue leads to inflammatory responses and endothelial cell dysfunction. *S*-Nitrosothiols have been shown to improve ischemia-reperfusion injury in various organs in animals (Konorev et al., 1996; Ikebe et al., 2000; Hallstrom et al., 2002; Mittermayr et al., 2003; Semsroth et al., 2005). We previously used SNO-α_1-PI as an *S*-nitrosothiol derivative to show that the cytoprotective effects of *S*-nitrosothiol may involve multiple mechanisms, including 1) maintenance of tissue blood flow; 2) induction of heme oxygenase-1, a cytoprotective enzyme; 3) suppression of neutrophil infiltration; and 4) reduction of apoptosis in the liver (Ikebe et al., 2000). The present study clearly showed that SNO-R410C also had a potent cytoprotective effect on ischemia-reperfusion liver injury, with its effect being stronger than that of SNO-HSA in this reperfusion model, despite its shorter in vivo half-life compared with that of SNO-HSA, as discussed below. Ikebe et al. (2000) observed that administration of GSNO had no cytoprotective effect. We found that the blood concentration of the SNO moiety after GSNO administration decreased very rapidly compared with that of SNO-HSA (Fig. 7). These findings suggest that sufficient half-life in the circulation of *S*-nitrosothiols is important for the cytoprotective effect. It remains unclear, however, whether mechanisms similar to those found for SNO-α_1-PI or alternative or additional ones may be involved in cytoprotection mediated by SNO-R410C.

Although *S*-nitroso levels in blood after administration of GSNO showed a transient increase and rapidly returned to the basal level, appreciable *S*-nitroso levels could be detected, even after 120 min, in blood of mice receiving SNO-R410C and SNO-HSA (Fig. 7). Experiments with radiolabeled proteins explained this result because carrier proteins that can escape renal excretion because of their large molecular size have a long half-life. However, we observed that R410C was more rapidly cleared from circulation than was HSA. A similar result was reported by Iwao et al. (2006): a single amino acid substitution at position 410 from arginine to alanine (R410A) shortened the half-life of the HSA mutant in circulation. It is of interest that *S*-nitrosylation improved the in vivo half-life of R410C, which may be because of the reduced liver uptake of SNO-R410C compared with that of R410C (Fig. 7; Table 1). All these findings indicate that using SNO-R410C can achieve prolonged delivery of NO, which is sufficient for in vivo biological activity.

In conclusion, our data suggest that SNO-R410C is not only a useful NO carrier but also a member of a new class of *S*-nitrosylated proteins possessing beneficial biological properties—antibacterial, antiapoptotic, and cytoprotective. Advantages of using SNO-R410C as an RNSO include 1) a high degree of *S*-nitrosylation, 2) physicochemical stability in solution and during lyophilization, 3) physiological degradation products (R410C and NO), and 4) sufficient half-life in circulation. Based on these advantages, we believe that further investigation in clinical settings is warranted.

Acknowledgments

We thank Judith B. Gandy for her excellent editing of our manuscript. We also thank Dr. Yuka Unno at the Center for Drug Discovery, Graduate School of Pharmaceutical Sciences, University of Shizuola, and Dr. Jun Yoshitake at the Yamagata Promotional Organization for Industrial Technology, for helpful discussions. We thank Dr. Teruo Akuta, at the Effector Cell Institute, Tokyo, and members of the Gene Technology Center in Kumamoto University for their important contributions to the experiments.

References

Akaike T (2000) Mechanisms of biological *S*-nitrosation and its measurement. *Free Radic Res* **33:**461–469.

Akaike T, Inoue K, Okamoto T, Nishino H, Otagiri M, Fujii S, and Maeda H (1997) Nanomolar quantification and identification of various nitrosothiols by high performance liquid chromatography coupled with flow reactors of metals and Griess reagent. *J Biochem (Tokyo)* **122:**459–466.

Bhattacharya AA, Grune T, and Curry S (2000) Crystallographic analysis reveals common modes of binding of medium and long-chain fatty acids to human serum albumin. *J Mol Biol* **303:**721–732.

Carter DC and Ho JX (1994) Structure of serum albumin. *Adv Protein Chem* **45:**153–203.

Chen RF (1967) Removal of fatty acids from serum albumin by charcoal treatment. *J Biol Chem* **242:**173–181.

Dworschak M, Franz M, Hallstrom S, Semsroth S, Gasser H, Haisjackl M, Podesser BK, and Malinski T (2004) *S*-Nitroso human serum albumin improves oxygen metabolism during reperfusion after severe myocardial ischemia. *Pharmacology* **72:**106–112.

Ewing JF, Young DV, Janero DR, Garvey DS, and Grinnell TA (1997) Nitrosylated bovine serum albumin derivatives as pharmacologically active nitric oxide congeners. *J Pharmacol Exp Ther* **283:**947–954.

Fang FC (2004) Antimicrobial reactive oxygen and nitrogen species: concepts and controversies. *Nat Rev Microbiol* **2:**820–832.

Foster MW, McMahon TJ, and Stamler JS (2003) *S*-Nitrosylation in health and disease. *Trends Mol Med* **9:**160–168.

Galliano M, Watkins S, Madison J, Putnam FW, Kragh-Hansen U, Cesati R, and Minchiotti L (1998) Structural characterization of three genetic variants of human serum albumin modified in subdomains IIB and IIIA. *Eur J Biochem* **251**:329–334.
Hallstrom S, Gasser H, Neumayer C, Fugl A, Nanobashvili J, Jakubowski A, Huk I, Schlag G, and Malinski T (2002) *S*-Nitroso human serum albumin treatment reduces ischemia/reperfusion injury in skeletal muscle via nitric oxide release. *Circulation* **105**:3032–3038.
Hess DT, Matsumoto A, Kim SO, Marshall HE, and Stamler JS (2005) Protein *S*-nitrosylation: purview and parameters. *Nat Rev Mol Cell Biol* **6**:150–166.
Hnatowich DJ, Layne WW, and Childs RL (1982) The preparation and labeling of DTPA-coupled albumin. *Int J Appl Radiat Isot* **33**:327–332.
Hogg N (2000) Biological chemistry and clinical potential of *S*-nitrosothiols. *Free Radic Biol Med* **28**:1478–1486.
Ikebe N, Akaike T, Miyamoto Y, Hayashida K, Yoshitake J, Ogawa M, and Maeda H (2000) Protective effect of *S*-nitrosylated alpha(1)-protease inhibitor on hepatic ischemia-reperfusion injury. *J Pharmacol Exp Ther* **295**:904–911.
Iwao Y, Anraku M, Yamasaki K, Kragh-Hansen U, Kawai K, Maruyama T, and Otagiri M (2006) Oxidation of Arg-410 promotes the elimination of human serum albumin. *Biochim Biophys Acta* **1764**:743–749.
Jaffrey SR, Erdjument-Bromage H, Ferris CD, Tempst P, and Snyder SH (2001) Protein *S*-nitrosylation: a physiological signal for neuronal nitric oxide. *Nat Cell Biol* **3**:193–197.
Katsumi H, Nishikawa M, Yamashita F, and Hashida M (2005) Development of polyethylene glycol-conjugated poly-*S*-nitrosated serum albumin, a novel *S*-nitrosothiol for prolonged delivery of nitric oxide in the blood circulation in vivo. *J Pharmacol Exp Ther* **314**:1117–1124.
Kim YM, Bombeck CA, and Billiar TR (1999) Nitric oxide as a bifunctional regulator of apoptosis. *Circ Res* **84**:253–256.
Konorev EA, Joseph J, Tarpey MM, and Kalyanaraman B (1996) The mechanism of cardioprotection by *S*-nitrosoglutathione monoethyl ester in rat isolated heart during cardioplegic ischaemic arrest. *Br J Pharmacol* **119**:511–518.
Kragh-Hansen U (1993) A micromethod for delipidation of aqueous proteins. *Anal Biochem* **210**:318–327.
Kragh-Hansen U, Campagnoli M, Dodig S, Nielsen H, Benko B, Raos M, Cesati R, Sala A, Galliano M, and Minchiotti L (2004) Structural analysis and fatty acid-binding properties of two Croatian variants of human serum albumin. *Clin Chim Acta* **349**:105–112.
Liu L and Stamler JS (1999) NO: an inhibitor of cell death. *Cell Death Differ* **6**:937–942.
Marks DS, Vita JA, Folts JD, Keaney JF Jr, Welch GN, and Loscalzo J (1995) Inhibition of neointimal proliferation in rabbits after vascular injury by a single treatment with a protein adduct of nitric oxide. *J Clin Investig* **96**:2630–2638.
Matsushita S, Isima Y, Chuang VT, Watanabe H, Tanase S, Maruyama T, and Otagiri M (2004) Functional analysis of recombinant human serum albumin domains for pharmaceutical applications. *Pharm Res (NY)* **21**:1924–1932.
Mittermayr R, Valentini D, Fitzal F, Hallstrom S, Gasser H, and Redl H (2003) Protective effect of a novel NO-donor on ischemia/reperfusion injury in a rat epigastric flap model. *Wound Repair Regen* **11**:3–10.
Miyamoto Y, Akaike T, Alam MS, Inoue K, Hamamoto T, Ikebe N, Yoshitake J, Okamoto T, and Maeda H (2000a) Novel functions of human alpha(1)-protease inhibitor after *S*-nitrosylation: inhibition of cysteine protease and antibacterial activity. *Biochem Biophys Res Commun* **267**:918–923.
Miyamoto Y, Akaike T, and Maeda H (2000b) *S*-Nitrosylated human alpha(1)-protease inhibitor. *Biochim Biophys Acta* **1477**:90–97.
Moncada S and Higgs A (1993) The L-arginine-nitric oxide pathway. *N Engl J Med* **329**:2002–2012.
Richardson G and Benjamin N (2002) Potential therapeutic uses for *S*-nitrosothiols. *Clin Sci (Lond)* **102**:99–105.
Semsroth S, Fellner B, Trescher K, Bernecker OY, Kalinowski L, Gasser H, Hallstrom S, Malinski T, and Podesser BK (2005) *S*-Nitroso human serum albumin attenuates ischemia/reperfusion injury after cardioplegic arrest in isolated rabbit hearts. *J Heart Lung Transplant* **24**:2226–2234.
Stamler JS, Jaraki O, Osborne J, Simon DI, Keaney J, Vita J, Singel D, Valeri CR, and Loscalzo J (1992) Nitric oxide circulates in mammalian plasma primarily as an *S*-nitroso adduct of serum albumin. *Proc Natl Acad Sci USA* **89**:7674–7677.
Sugio S, Kashima A, Mochizuki S, Noda M, and Kobayashi K (1999) Crystal structure of human serum albumin at 2.5 A resolution. *Protein Eng* **12**:439–446.
Yamaoka K, Tanigawara Y, Nakagawa T, and Uno T (1981) A pharmacokinetic analysis program (multi) for microcomputer. *J Pharmacobiodyn* **4**:879–885.
Yamasaki Y, Sumimoto K, Nishikawa M, Yamashita F, Yamaoka K, Hashida M, and Takakura Y (2002) Pharmacokinetic analysis of in vivo disposition of succinylated proteins targeted to liver nonparenchymal cells via scavenger receptors: importance of molecular size and negative charge density for in vivo recognition by receptors. *J Pharmacol Exp Ther* **301**:467–477.

Address correspondence to: Masaki Otagiri, Department of Biopharmaceutics, Graduate School of Pharmaceutical Sciences, Kumamoto University, 5-1 Oe-honmachi, Kumamoto 862-0973, Japan. E-mail: otagirim@gpo.kumamoto-u.ac.jp

Available online at www.sciencedirect.com
ScienceDirect
International Journal of Pharmaceutics 329 (2007) 19–24
INTERNATIONAL JOURNAL OF PHARMACEUTICS
www.elsevier.com/locate/ijpharm

The role of *N*-acetyl-methioninate as a new stabilizer for albumin products

Makoto Anraku [a], Yousuke Kouno [a], Toshiya Kai [a,b], Yasufumi Tsurusaki [a], Keishi Yamasaki [a], Masaki Otagiri [a,*]

[a] *Department of Biopharmaceutics, Graduate School of Pharmaceutical Sciences, Kumamoto University, 5-1 Oe-honmachi, Kumamoto 862-0973, Japan*
[b] *Pharmaceutical Research Center, Nipro Corporation, 3023 Nojicho, Kusatsu, Shiga 525-0055, Japan*

Received 13 April 2006; received in revised form 5 August 2006; accepted 12 August 2006
Available online 17 August 2006

Abstract

Sodium octanoate (Oct) and *N*-acetyl-L-tryptophanate (*N*-AcTrp) are widely used as stabilizers during the pasteurization of albumin products. However, *N*-AcTrp has a possible side effect of intracerebral disease. To provide safe and risk-free albumin products, we validated *N*-acetyl-methioninate (*N*-AcMet) as a new stabilizer for albumin products. The effect of *N*-AcMet on oxidation was examined using 2,2′-azobis(2-amidinopropane) dihydrochloride (AAPH) as an oxidizing agent. Carbonyl content in the presence of *N*-AcMet, as well as that in the presence of *N*-AcTrp after 24 h (Anraku et al., 2004), was significantly decreased. The effect of AAPH on the oxidative status of 34-Cys on human serum albumin was also studied by HPLC. It was found that *N*-AcMet as well as *N*-AcTrp, has a large protective effect on the sulfhydryl group after 1 h. Further, *N*-AcMet was found to be a superior radical scavenger to *N*-AcTrp using 1,1′-diphenyl-2-picrylhydrazyl (DPPH) radicals. The thermal stabilizing role of *N*-AcMet manifested as an increase in denaturation temperature and calorimetric enthalpy, as determined by differential scanning calorimetry (DSC). In the present study, we suggest that use of *N*-AcMet in albumin preparation is safe and free of risk of side effects.

Keywords: Albumin; Sulfhydryl groups; Calorimetry (DSC); Antioxidant activity; *N*-Acetyl-L-methioninate; Oxidation

1. Introduction

Human serum albumin (HSA) is the most abundant protein in plasma, and in addition to being the primary colloid, it serves as an important transport and depot protein (Peters, 1996). Large amounts of albumin are used clinically during surgery and to treat shock trauma. As the only source of HSA for clinical application is donated human blood, the risk of transmitting pathogenic viruses, such as those causing hepatitis, HIV, and as yet unidentified diseases, exists. Pasteurization of HSA is carried out by heating at 60 °C for several hours with sodium octanoate (Oct) and *N*-acetyl-L-tryptophanate (*N*-AcTrp) as commonly used stabilizers (Shrake et al., 1984; Ross et al., 1984), a process that usually destroys the viruses present. These commonly used additives effectively protect HSA by increasing the melting temperature as determined by differential scanning calorimetry (DSC) and decreasing the formation of aggregates after heating (Arakawa and Kita, 2000). We have previously shown that Oct has the greatest stabilizing effect against heat, while *N*-AcTrp diminishes oxidation of HSA (Anraku et al., 2004). However, *N*-AcTrp has a possible side effect of intracerebral disease (Aguilera et al., 2001). In Trp metabolism, 3-hydroxykynurenine is known to have particularly strong neurotoxic properties (Topczewska-Bruns et al., 2003), and the accumulation of Trp metabolites in nervous tissue due to HSA product administration may be involved in pathogenesis of several neurological disorders in uremia. To provide safe and risk-free albumin preparations, it is important to find new stabilizing reagents instead of *N*-AcTrp.

All amino acid residues of proteins are susceptible to oxidative modification by one or more forms of reactive oxygen species (ROS) (Vogt, 1995; Brot and Weissbach, 1983). The oxidative modifications of sulfur-containing amino acids such as cysteine and methionine (Met) could serve as antioxidants via their cyclic oxidation and reduction. In particular, Met residues of proteins are susceptible to oxidation by almost all forms of ROS (Vogt, 1995). On the other hand, no effect on oxidation was found for *N*-acetyl-cysteinate in our previous studies, although cysteine (Cys) residues of proteins are susceptible to oxidation (Anraku et al., 2004). Thus, we focused on a sulfur-containing

* Corresponding author. Tel.: +81 96 370 4150; fax: +81 96 362 7690.
E-mail address: otagirim@gpo.kumamoto-u.ac.jp (M. Otagiri).

0378-5173/$ – see front matter © 2006 Elsevier B.V. All rights reserved.
doi:10.1016/j.ijpharm.2006.08.014

amino acid having mercapto groups, *N*-acetyl-methioninate (*N*-AcMet).

In the present study, we investigated the protective effect of *N*-AcMet on the oxidation of albumin. In addition, we investigated the stabilizing effect of *N*-AcMet by differential scanning calorimetry (DSC). We suggest that the co-use of *N*-AcMet and Oct produces an excellent stabilizing effect on albumin and depresses agglomeration safely and without any risk of side effects.

2. Materials and methods

2.1. Materials

HSA donated by Chemo-Sera-Therapeutic Research Institute (Kumamoto, Japan) and genetically recombinant human serum albumin (rHSA) donated by Nipro Corporation (Shiga, Japan) were defatted using charcoal treatment as described by Chen (1967). After dialysis against distilled water, the protein fraction was freeze-dried and stored at −20 °C until use. While HSA was used for all the experiments, rHSA was used only for the expected examination for the clinical application. *N*-Acetyl-L-methioninate (*N*-AcMet) and *N*-acetyl-L-tryptophanate (*N*-AcTrp), were purchased from Nacalai Tesque (Kyoto, Japan). Fluoresceinamine (isomer II) and sodium octanoate (Oct) were purchased from Sigma Chemical Co. (St. Louis, MO). 2,2′-Azobis(2-amidino-propane)dihydrochloride (AAPH) and 1,1′-diphenyl-2-picrylhydrazyl (DPPH) were purchased from Nacalai Tesque (Kyoto, Japan).

2.2. Methods

2.2.1. Effect of oxidation on HSA in the presence and absence of ligands

HSA (50 μM), with and without (250 μM) additives, was oxidized by exposure to AAPH (10 mM) in 67 mM sodium phosphate buffer (pH 7.4, 37 °C), as described by Niki (1987). After incubation for 1 or 24 h, oxidation was stopped by the addition of acetone. Protein carbonyl content was determined using the method of Climent et al. (1989). The carbonyl groups were derivatized with fluoresceinamine and their numbers were calculated from the absorbancy of the complexes at 490 nm (Jasco Ubest-35 UV–vis spectrophotometer). Mercaptalbumin (HMA; reduced form) and nonmercaptalbumin (HNA-1 and -2; oxidized forms) were separated by application to an HPLC-column packed with *N*-methylpyridinium polymer cross-linked with ethylene glycol dimethacrylate, prepared as described previously (Sugii et al., 1989; Narazaki et al., 1997). From the HPLC profiles of HSA, the values of each albumin fractions (f(HMA), f(HNA-1), and f(HNA-2)) were estimated by dividing the area of each fraction by the total area corresponding to HSA.

2.2.2. Scavenging of DPPH (1,1′-diphenyl-2-picrylhydrazyl) radicals in solution

Radical scavenging activity of *N*-AcMet and *N*-AcTrp was tested in ethanolic solution (10 ml of ethanol, 10 ml of 50 mM 2-(*N*-morpholino)ethanesulfonic acid (MES) buffer (pH 5.5) and 5 ml of 0.5 mM DPPH in ethanol) with an albumin concentration of 50 μM and a ligand concentration of 250 μM. Radical scavenging was estimated from the decrease in absorbance of DPPH radicals at 517 nm due to scavenging of an unpaired electron from stable DPPH radicals by ligands (Kogure et al., 1999).

2.2.3. Effect of heating on HSA in the presence and absence of ligands

Differential scanning calorimetry (DSC) was carried out on HSA with a protein concentration of 0.1 mM in 67 mM sodium phosphate buffer, pH 7.4 using a MicroCal MC-2 ultrasensitive DSC (MicroCal Inc., Northampton, MA) with a heating rate of 1 K/min. The calorimetric reversibility of the thermally induced transition was checked by reheating the cooled protein solution from the first run in the calorimetric cell, which was flushed with nitrogen. The results showed, as was also observed by Picó (1997), that heating to or above 85 °C causes irreversible denaturation. The data obtained from DSC were applied to non-linear fitting algorithms to calculate thermodynamic parameters of thermal denaturation temperature (T_m), calorimetric enthalpy (ΔH_{cal}) and van't Hoff enthalpy (ΔH_v), and analyzed by Using Origin™ scientific plotting software to determine C_p from the temperature dependence of excess molar heat capacity. Each sample was recorded before heating and after heating to 60 °C for 30 min.

2.2.4. Thermal stabilities on HSAs in the presence and absence of N-AcMet for clinical application

Aqueous solutions (25%, w/v) were prepared by dissolving HSA and rHSA in 500 ml physiological saline. Then, stabilizers Oct (1662 mg) and *N*-AcMet (1912.5 mg) were added and dissolved, and 50-ml aliquots of HSA or rHSA solutions were hermetically sealed in 50-ml vials. The samples were subjected to heat treatment under pasteurization conditions of 60 °C for 30 min, and the generation of contaminants was observed.

2.2.5. Statistics

Statistical significance was evaluated using ANOVA followed by the Newman–Keuls method for comparisons of more than two means. A value of $p < 0.05$ was regarded as statistically significant. Results are reported as mean ± S.D.

3. Results

3.1. Effect of oxidation on HSA in the presence and absence of ligands

HSA exposed to AAPH results in the formation of carbonyl groups. The carbonyl content of HSA, which has not been exposed to AAPH, was 0.037 ± 0.002 mol/mol protein for all the samples ($n = 3$). It is evident from Fig. 1 that the carbonylation increased with incubation time. The presence of Oct has no inhibiting effect on carbonyl formation after 1 hr exposure to AAPH, while *N*-AcMet had a protective effect against prolonged exposure to the oxidant. Similar results were also observed for